Microarray Expression Analyses of Arabidopsis Guard Cells and Isolation of a Recessive Abscisic Acid Hypersensitive Protein Phosphatase 2C Mutant [W]

Nathalie Leonhardt,[1,2] June M. Kwak,[1,3] Nadia Robert, David Waner, Guillaume Leonhardt, and Julian I. Schroeder[4]

Cell and Developmental Biology Section, Division of Biological Sciences, and Center for Molecular Genetics, University of California, San Diego, La Jolla, California 92093-0116

Oligomer-based DNA Affymetrix GeneChips representing about one-third of Arabidopsis (*Arabidopsis thaliana*) genes were used to profile global gene expression in a single cell type, guard cells, identifying 1309 guard cell–expressed genes. Highly pure preparations of guard cells and mesophyll cells were isolated in the presence of transcription inhibitors that prevented induction of stress-inducible genes during cell isolation procedures. Guard cell expression profiles were compared with those of mesophyll cells, resulting in identification of 64 transcripts expressed preferentially in guard cells. Many large gene families and gene duplications are known to exist in the Arabidopsis genome, giving rise to redundancies that greatly hamper conventional genetic and functional genomic analyses. The presented genomic scale analysis identifies redundant expression of specific isoforms belonging to large gene families at the single cell level, which provides a powerful tool for functional genomic characterization of the many signaling pathways that function in guard cells. Reverse transcription–PCR of 29 genes confirmed the reliability of GeneChip results. Statistical analyses of promoter regions of abscisic acid (ABA)–regulated genes reveal an overrepresented ABA responsive motif, which is the known ABA response element. Interestingly, expression profiling reveals ABA modulation of many known guard cell ABA signaling components at the transcript level. We further identified a highly ABA-induced protein phosphatase 2C transcript, *AtP2C-HA*, in guard cells. A T-DNA disruption mutation in *AtP2C-HA* confers ABA-hypersensitive regulation of stomatal closing and seed germination. The presented data provide a basis for cell type–specific genomic scale analyses of gene function.

INTRODUCTION

In the leaf epidermis, pairs of guard cells form stomatal pores, which provide CO_2 intake conduits for photosynthesis and sites for controlling transpirational water loss in plants. The guard cell system has been adapted and developed for studying the transduction of environmental and endogenous signals in plants because guard cells cell-autonomously respond to stimuli such as blue light, temperature, CO_2, drought, abscisic acid (ABA), and other hormones. Moreover, models have been developed allowing individual mechanisms and branches in early signaling to be characterized with mechanistic and temporal resolu-

tion (reviewed in MacRobbie, 1998; Schroeder et al., 2001; Finkelstein et al., 2002).

During drought, the phytohormone ABA triggers cellular responses resulting in stomatal closing, thus reducing plant water loss. Characterization of guard cell–expressed genes on a genomic scale would greatly facilitate identification of new ABA and other signal transduction mechanisms because guard cells can be probed at different steps and branches within early signal transduction cascades (Mäser et al., 2003). Furthermore, only recently genomic studies have been reported to examine which genes are expressed in a single plant cell type (Becker et al., 2003; Birnbaum et al., 2003; Honys and Twell, 2003), largely because of the fact that it is not easy to obtain a large amount of a single purified cell type from Arabidopsis (*Arabidopsis thaliana*). An initial EST sequencing study previously reported ~500 guard cell–expressed sequence tags in *Brassica campestris* (Kwak et al., 1997). Expression profiling in Arabidopsis has been used to obtain valuable information on functions of genes under a variety of conditions (Harmer et al., 2000; Wang et al., 2000; Hugouvieux et al., 2001; Chen et al., 2002). However, expression analyses in plants and other systems have thus far focused on whole organs (Schena et al., 1995; Harmer et al., 2000; Perez-Amador et al., 2001; Seki et al., 2001, 2002; Hoth et al., 2002; Yin et al., 2002).

Only a few genes have been cloned from recessive ABA-insensitive mutants (Giraudat et al., 1992; Finkelstein, 1994; Finkelstein and Lynch, 2000; Lopez-Molina and Chua, 2000;
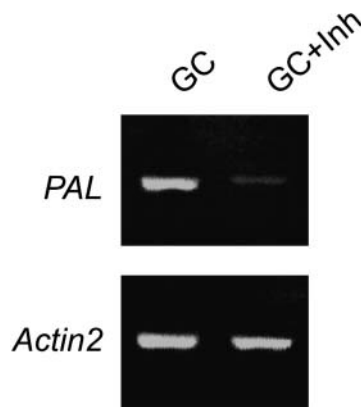
Figure 1. Transcription Inhibitors Suppress Stress-Induced *PAL* Gene Expression during Guard Cell Isolation.

RT-PCR analyses of *PAL* in guard cells extracted in the absence (GC) or presence (GC + Inh) of the transcription inhibitors actinomycin D (33 mg/L) and cordycepin (100 mg/L). The *Actin2* gene was amplified as a control.

Wang et al., 2001; Kwak et al., 2002, 2003; Mustilli et al., 2002; Zhu et al., 2002). In addition, several negative regulators of ABA signaling, which produce ABA hypersensitivity when mutated, have been characterized (Cutler et al., 1996; Pei et al., 1998; Lu and Fedoroff, 2000; Hugouvieux et al., 2001; Lee et al., 2001; Merlot et al., 2001; Xiong et al., 2001a, 2001b). However, conventional genetic screens have left large portions of plant signal transduction networks uncharacterized, which is likely because of redundancy within plant gene families. Genetic analysis of redundant pathways requires the study of double or multiple mutants. Unfortunately, this is impractical for large gene families. For example, for the ~69 protein phosphatase 2C (PP2C) genes expressed in Arabidopsis, 2346 distinct double mutant combinations could be generated for phenotypic analyses. This could partly explain why no recessive PP2C knockout mutant phenotypes have yet been reported in plants, with the exception of intragenic suppressor mutations (Merlot et al., 2001).

Given the substantial number of large gene families found in plants, gaining knowledge of the expression of specific gene family members in individual cell types will provide a powerful single cell–type genomic approach to identifying which members of a gene family are likely to function in a specific pathway. For instance, the *RCN1* protein phosphatase 2A subunit and the redundant NADPH oxidase *AtrbohD* and *AtrbohF* genes were shown to function in early ABA signal transduction by initially revealing high expression levels of these genes in guard cells (Kwak et al., 2002, 2003). The combined analysis of guard cell–specific expression profiles with phenotypic analysis of Arabidopsis knockout mutants of homologous gene family members will allow the functional identification of redundant and unknown genes that play important roles in plant signal transduction.

In an effort to provide genomic scale information on gene expression in a single cell type, we identify transcripts expressed in Arabidopsis guard cells, compare these with expression in whole leaf mesophyll tissues, and report their regulation by ABA. In addition, our results provide new information on *cis*-elements conferring gene regulation by ABA. Interestingly, a current working model for early ABA signal transduction is presented, unexpectedly demonstrating that ABA modulates the mRNA levels of many known negatively regulating and positively transducing ABA signal transduction mechanisms in guard cells. Additionally, to demonstrate the utility of these expression profile analyses, one PP2C gene, *AtP2C-HA*, which is strongly induced by ABA in guard cells, was selected. T-DNA disruption of *AtP2C-HA* confers ABA-hypersensitive regulation of both stomatal closing and seed germination. These results show that this cell type–oriented genomic scale approach is a powerful tool for identifying new signal transduction mechanisms.

RESULTS

To establish a genomic scale analysis of gene function in guard cells, we performed expression-profiling experiments using Affymetrix GeneChips, representing ~8100 genes in the Arabidopsis genome. Experiments were performed over the course of 18 months. Four- to five-week-old Arabidopsis (Columbia) plants were either control treated or treated with 100 μM ABA for 4 h, and guard cells and mesophyll cells were extracted at the same time from plants grown in parallel. Total RNA was prepared for individual microarray hybridizations from control and ABA-treated guard cells for each of the three experiments and from control and ABA-treated mesophyll cells for two of the three experiments (one mesophyll hybridization failed), resulting in three pairs of guard cell hybridizations and two pairs of mesophyll cell hybridizations (for a total of 10 microarray hybridizations). In addition, for each individual hybridization, three RNA samples from three independent cell preparations were extracted and pooled (a total of 30 independent RNA extractions) (Excel files reporting expression data for all 10 experiments are available as supplemental data online and at http://www-biology.ucsd.edu/labs/schroeder/guardcellchips. html). For each microarray, overall intensity normalization for the entire probe set was performed as described by Zhu et al. (2001). Then, for each probe set, the signal value, which assigns a relative measure of abundance to the transcript, and the detection P-value, which indicates whether a transcript is reliably detected, were calculated from each independent guard cell and mesophyll cell hybridization (see Methods).

Effect of Transcription Inhibitors on Stress-Inducible Genes

To inhibit the modulation of gene expression in response to stress during physical isolation and enzymatic digestions for guard cell and mesophyll cell protoplast preparations, two transcription inhibitors, actinomycin D and cordycepin, were applied during all steps of protoplast extraction. To test whether these inhibitors suppressed induction of stress-inducible genes, reverse transcription (RT)–PCR was performed using cDNA synthesized from guard cell RNA from protoplasts prepared in the presence or absence of these inhibitors.

Phe ammonia-lyase (*PAL*) gene mRNA levels were used to monitor the effect of the inhibitors because *PAL* gene expression
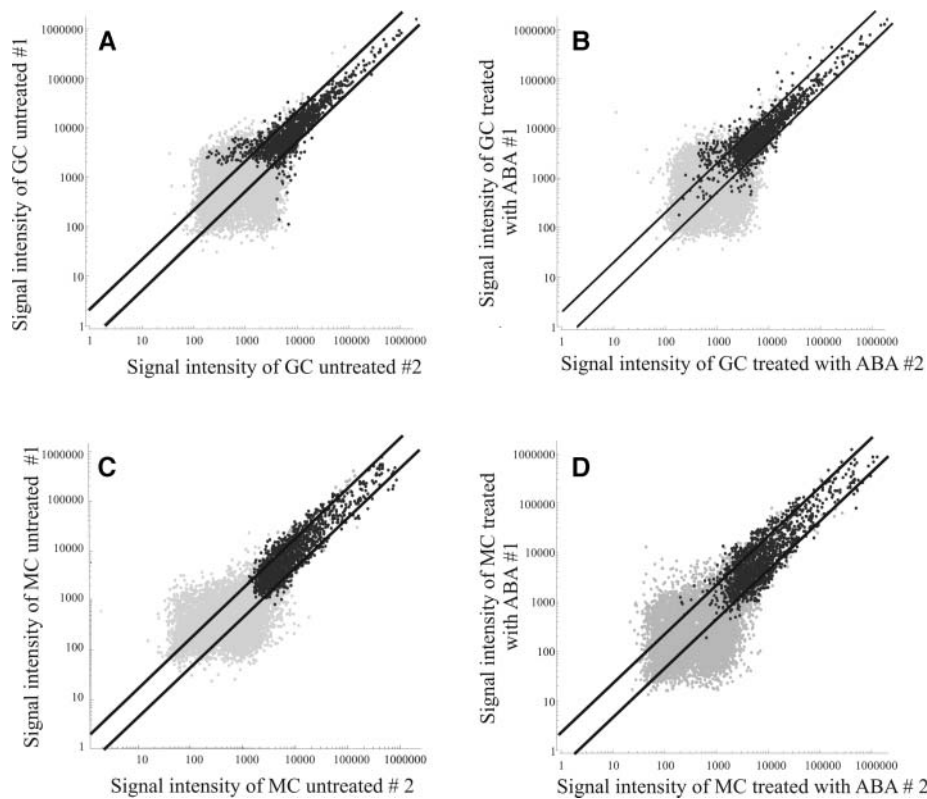
Figure 2. GeneChip Hybridizations Show Genomic Scale Reproducibility.

Scatter plots comparing the raw signal intensities of two independent experiments from guard cells **(A)**, guard cells treated with ABA **(B)**, mesophyll cells **(C)**, and mesophyll cells treated with ABA **(D)**. Each gene is represented by one dot. For each gene, the raw RNA expression level in one experiment is given on the *x* axis, and the expression level for the same gene in the other experiment is plotted on the *y* axis. The solid diagonal lines indicate a difference by a factor of 2 between the two hybridizations for visual reference. Significantly expressed genes detected as Present or Marginal in two or three samples (see Methods) are represented by black dots, whereas genes for which expression levels were not significant in two or three samples are shown as gray dots.

is induced by stress (Wanner et al., 1995). As shown in Figure 1, expression of *PAL* was highly induced in guard cells prepared in the absence of transcription inhibitors. By contrast, *PAL* expression was low in guard cells prepared in the presence of transcription inhibitors. Similar results were observed for other stress-inducible genes, including *COR47*, genes encoding heat shock proteins (At5g04140 and At1g16030), and glutathione *S*-transferase (At5g02200) (data not shown). Thus, inhibitors of transcription suppressed stress-inducible gene induction during cell isolations.

Reproducibility of Chip Hybridizations

To test the variability between our chip hybridization experiments, raw signal intensities from all probe sets were plotted for all possible pairs of independent experiments. Scatter plots of the raw data for the control-treated guard cells, ABA-treated guard cells, control-treated mesophyll cells, and ABA-treated mesophyll cells are shown in Figure 2. The diagonal lines in Figure 2 indicate twofold relative intensity differences between two experiments. These scatter plots show that the majority

(>90%) of the significantly expressed genes fall between the two lines, showing that most genes exhibit less than twofold variation in signal intensity between the two independent chip hybridizations, even though individual mRNA isolations were performed over a period of 18 months. This level of reproducibility is likely attributed to tightly controlled growth and experimental conditions. However, some genes with low raw signal intensities corresponding to either noise or low abundance mRNAs showed more variability (Figure 2, gray points). The same comparisons were performed with the other samples against each other (see Supplemental Figure 1 online).

Functional Classification of Genes Expressed in Guard Cells and Mesophyll Cells

Among the >8100 genes analyzed, 1309 transcripts were found to be significantly expressed in guard cells and 1479 in mesophyll cells (see Supplemental Tables 1 and 2 online). A previously reported (Ghassemian et al., 2001) and recently further enhanced annotation of the genes represented on the GeneChip was used
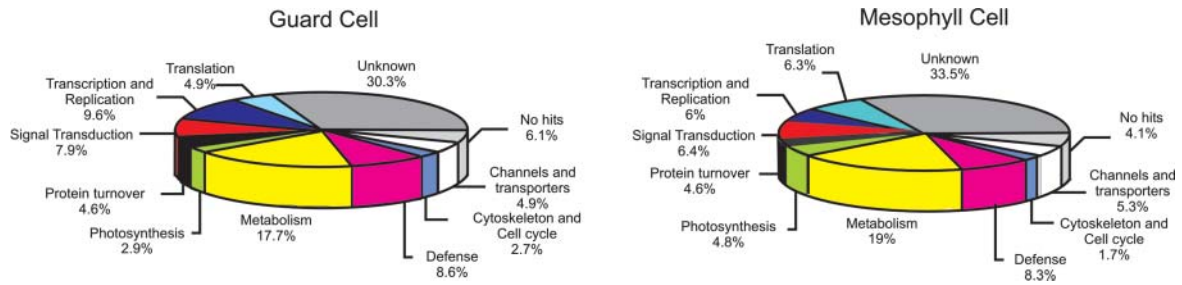
Figure 3. Comparison of Predicted Functional Distribution of Guard Cell– and Mesophyll Cell–Expressed Genes Shows a Higher Relative Portion of Photosynthesis Gene Expression in Mesophyll Cells.

Distribution of guard cell and mesophyll cell profiles among 11 major classes was performed using the MIPS database (http://mips.gsf.de/proj/thal/db/tables/tables_func_frame.html).

for analyses (see supplemental data online and http://www-biology.ucsd.edu/labs/schroeder/index.html, click on Gene-chip). We classified these genes according to their putative functions based on the classification of the Munich Information Center for Protein Sequence (MIPS) database to determine whether these specialized cells allocate gene expression patterns differently among classifications.

Figure 3 shows a summary of the functional categorization of the transcripts detected in guard cells and mesophyll cells, showing that the majority of the known genes are predicted to function in metabolic pathways, followed by genes implicated in transcription and replication and signal transduction in both guard cells and mesophyll cells. Interestingly, the percentage of genes in each category is similar between the two cell types, with some exceptions, including photosynthesis-related genes with 4.8% in mesophyll cells and 2.9% in guard cells. This correlates with the fact that mesophyll cells possess the major photosynthetic activity in leaves.

Identification of Genes Preferentially Expressed in Guard Cells

To identify genes expressed preferentially in guard cells compared with mesophyll cells, scatter plots of guard cell versus mesophyll cell expression were generated. As shown in Figure 4, many guard cell–expressed genes are also expressed in mesophyll cells. These data provide experimental support for the prediction that ∼60 to 77% of plant genes do not have a strict tissue-specific expression (Okamura and Goldberg, 1989).

Interestingly, guard cell versus mesophyll cell analyses revealed that only 64 transcripts were detectable solely in guard cells in all three independent guard cell chip hybridizations compared with the two independent mesophyll chip hybridizations. These genes encode transcription factors, signal transduction proteins such as protein kinases, receptor protein kinases, and metabolic pathway proteins (Table 1). Among these genes, several have been reported previously to be predominantly expressed in guard cells, indicating the reliability of the method. These include *ECERIFERUM2* (*CER2*) that functions in cuticular wax accumulation. *CER2* is expressed in guard cells and trichomes but not in mesophyll cells (Xia et al., 1997). The *KAT1* gene encoding an inward-rectifying K$^+$ channel (Anderson et al., 1992; Schachtman et al., 1992) has also been reported to be expressed predominantly in guard cells (Nakamura et al., 1995). Importantly, we also identified previously uncharacterized genes that are preferentially expressed in guard cells and thus are strong candidates for contributing to guard cell signal transduction and development. Many of these highly expressed genes encode proteins of unknown function and therefore may be of particular interest for future studies (Table 1).

Identification of Genes Regulated by ABA

To identify genes regulated by ABA in guard cells and/or in mesophyll cells, six groups with distinct expression profiles were

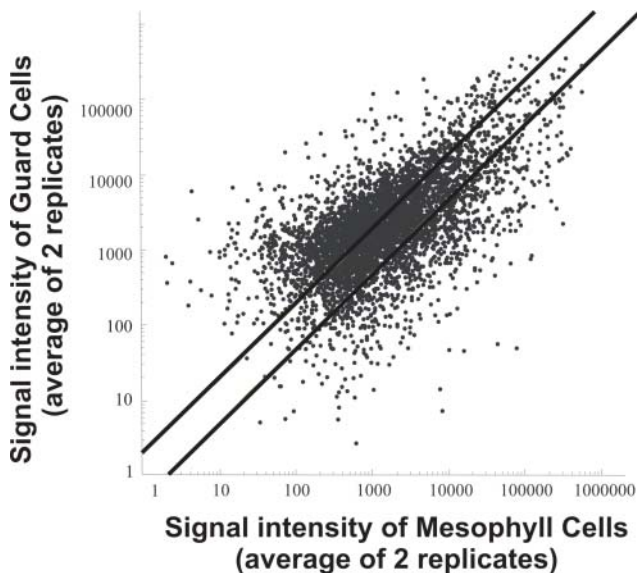**Figure 4.** Comparison of Guard Cell–Expressed Genes versus Mesophyll Cell–Expressed Genes.

Scatter plot of the normalized signal intensity values from guard cell versus mesophyll cell comparison (average of two and three replicates for mesophyll cells and guard cells, respectively) shows that many genes are expressed in both guard cells and mesophyll cells, albeit many at substantially different levels.

Table 1. Genes Preferentially Expressed in Guard Cells

Affy Probe[a]	Description	AGI Number[b]	Experiment 1		Experiment 2		Experiment 3	
			Signal Value[c]	P-Value[d]	Signal Value	P-Value	Signal Value	P-Value
12100_at	MYB family transcription factor	At2g21650	3,851	0.04397	7,039	0.00653	4,685	0.00869
12188_at	Unknown protein	At2g28870	6,782	0.03937	7,601	0.02187	3,274	0.03937
12196_at	Unknown protein	At2g28410	5,143	0.03934	6,363	0.00999	3,333	0.00114
12261_at	Receptor kinase	At1g11340	18,071	0.00039	20,116	0.00160	24,685	0.00067
12284_at	Somatic embryogenesis receptor-like kinase	At1g34210	7,252	0.00486	13,534	0.00307	10,207	0.00056
12448_at	Acyl-CoA synthetase	At2g47240	3,761	0.01145	4,334	0.01145	2,148	0.01494
12493_g_	Chloride channel	At5g49890	4,235	0.03516	6,627	0.00189	2,519	0.01309
12499_at	Phosphatidylinositol/ phosphatidylcholine transfer protein	At2g16380	9,010	0.00754	5,813	0.02786	1,780	0.00114
12780_s_	Unknown protein	At4g10840	9,242	0.00486	10,923	0.00223	21,807	0.00114
12796_s_	β-Ketoacyl-CoA synthase	At2g26250	36,481	0.00189	40,054	0.00067	91,193	0.00022
12959_at	Ser/Thr protein kinase	At2g32850	8,793	0.01930	4,356	0.04397	1,139	0.10730
13110_at	Symbiosis-related protein	At4g04620	18,390	0.02471	11,383	0.02471	15,203	0.00039
13179_at	Unknown protein	At2g43680	6,676	0.00754	11,499	0.00039	9,828	0.00081
13482_at	Nodulin-like protein	At2g37450	9,952	0.00869	17,055	0.00135	11,928	0.00869
13554_at	β-Ketoacyl-CoA synthase	At2g16280	41,511	0.00094	39,345	0.01157	89,871	0.00074
13577_s_	CER2	At4g24510	37,080	0.00586	45,432	0.00195	80,154	0.00586
13612_at	Ubiquitin-conjugating enzyme	At2g16740	6,194	0.03516	2,892	0.02786	4,891	0.00223
14048_at	Protein kinase	At2g18890	7,378	0.04397	4,701	0.04397	4,578	0.00869
14527_at	Unknown protein	At2g30500	7,794	0.01930	4,417	0.04397	2,668	0.00307
14663_s_	Glycosyl hydrolase	At4g24040	6,918	0.01930	6,836	0.00486	4,016	0.00564
14664_i_	Trehalose-6-phosphate synthase	At1g78580	4,641	0.03516	3,586	0.00081	3,987	0.00032
14665_r_	Trehalose-6-phosphate synthase	At1g78580	7,050	0.01494	7,118	0.03516	4,178	0.00262
14712_s_	Translation initiation factor	At5g43810	5,681	0.00653	8,440	0.03516	2,845	0.01700
14870_at	Auxilin-like protein	At1g21660	4,453	0.03516	4,310	0.02187	2,089	0.03516
15034_at	Unknown protein	At2g39340	10,976	0.00096	9,830	0.00999	26,291	0.00027
15187_s_	Fimbrin 2	At5g48460	3,705	0.03937	3,067	0.01494	1,538	0.03516
15251_at	No hits		55,883	0.00022	66,764	0.00022	93,068	0.00022
15368_at	Unknown protein	At4g14830	45,332	0.00032	51,212	0.00022	43,714	0.00027
15389_at	Unknown protein	At2g22860	9,290	0.00307	10,139	0.00359	15,106	0.00032
15528_at	Electron transfer flavoprotein-ubiquinone oxidoreductase	At2g43400	9,730	0.01494	6,377	0.01145	4,914	0.00189
15548_at	Unknown protein	At1g11820	6,745	0.02187	7,496	0.00160	15,819	0.00032
15550_at	Unknown protein	At1g15200	5,624	0.01494	5,624	0.01145	4,719	0.00307
15642_at	Unknown protein	At1g68530	10,249	0.00358	7,315	0.00223	10,099	0.00081
15695_s_	Histone H1	At2g18050	5,054	0.03134	5,267	0.02187	1,873	0.00999
15709_at	Protein kinase	At1g62400	18,377	0.00135	18,227	0.00359	17,259	0.00067
15835_at	NAM (no apical meristem)-like protein	At2g02450	8,368	0.00160	14,219	0.00189	6,552	0.00096
16092_s_	Potassium channel protein KAT1	At5g46240	12,663	0.04397	17,358	0.00114	17,941	0.00022
16148_s_	Kinesin-like protein	At5g54670	15,495	0.03937	12,073	0.00032	17,155	0.00039
16161_s_	Gly-rich protein (AtGRP2)	At2g21060	56,617	0.00027	42,066	0.00160	74,085	0.00022
16403_at	ADP-glucose pyrophosphorylase	At2g21590	20,298	0.00261	12,647	0.00564	13,381	0.00223
16453_s_	Histone	At1g06760	5,961	0.00754	4,816	0.02471	2,732	0.00653
16567_s_	Unknown protein	At2g47980	6,685	0.00869	8,013	0.02187	2,120	0.03516
16624_s_	Transcription factor	At1g08810	6,792	0.03516	4,895	0.03516	8,108	0.00189
17143_s_	Unknown protein	At2g38300	7,847	0.00564	6,204	0.00999	12,622	0.00096
17386_at	Pro-rich protein	At2g21140	5,524	0.04900	4,479	0.00262	6,674	0.00039
17518_s_	Transcriptional regulator	At3g26790	5,288	0.00754	3,076	0.00359	2,588	0.00039
17539_at	Nuclear cap binding protein CBP20	At5g44200	5,628	0.03516	3,657	0.01145	4,012	0.01700
17567_at	Unknown protein	At5g03540	9,045	0.02187	8,730	0.00067	25,037	0.00027

(Continued)

Table 1. (continued).

Affy Probe[a]	Description	AGI Number[b]	Experiment 1		Experiment 2		Experiment 3	
			Signal Value[c]	P-Value[d]	Signal Value	P-Value	Signal Value	P-Value
17902_s_	Unknown protein	At2g35330	10,193	0.00047	9,572	0.00160	11,924	0.00027
18319_g_	Transcription factor ZAP1	At2g04880	3,044	0.05447	7,593	0.00223	3,729	0.00096
18478_at	Receptor protein kinase	At1g78530	12,521	0.00564	9,739	0.01930	9,218	0.00056
18522_at	Kinase-like protein	At4g14480	12,486	0.00114	14,055	0.00754	20,933	0.00027
18625_at	Unknown protein	At1g03290	4,489	0.05444	2,519	0.03937	6,282	0.00486
18663_s_	Unknown protein	At4g24130	7,330	0.05447	15,540	0.00262	13,017	0.00067
18918_at	No hits		6,232	0.01700	6,271	0.00999	6,302	0.00135
18953_at	Branched-chain alpha-keto acid dehydrogenase	At1g21400	6,569	0.02786	5,540	0.04900	4,649	0.01494
18975_g_	Protein kinase	At4g35780	6,382	0.01700	6,307	0.00418	4,428	0.00754
19008_s_	Glycosyl hydrolase	At2g28470	20,096	0.00486	28,800	0.00418	29,361	0.00032
19365_s_	Cinnamyl-alcohol dehydrogenase	At4g39330	7,367	0.01930	6,090	0.00307	9,559	0.00022
19439_at	Aldehyde dehydrogenase protein	At4g36250	3,851	0.04397	7,039	0.00653	4,685	0.00869
19948_at	Unknown protein	At2g31580	6,782	0.03937	7,601	0.02187	3,274	0.03937
20067_at	Unknown protein	At2g04280	5,143	0.03934	6,363	0.00999	3,333	0.00114
20129_at	Pyrophosphate–fructose-6-phosphate 1-phosphotransferase	At2g22480	18,071	0.00039	20,116	0.00160	24,685	0.00067
20518_at	Unknown protein	At1g10060	7,252	0.00486	13,534	0.00307	10,207	0.00056
20570_at	Trehalose-6-phosphate phosphatase	At4g12430	3,761	0.01145	4,334	0.01145	2,148	0.01494

[a] Describes names of probe set on Affymetrix chip.
[b] AGI locus numbers.
[c] Signal value, which assigns a relative measure of abundance of transcript of each gene.
[d] Detection P-value, which indicates whether a transcript is reliably detected.

analyzed based on cluster analyses (see Methods) and are shown in Figure 5. The number of genes found in each cluster will depend on the applied statistical algorithms and parameters. Group I contains 21 transcripts that are ABA induced in both guard cells and mesophyll cells (Table 2, Figures 5A and 5B). This group includes several known genes that were shown previously to be induced by ABA in different tissues, including dehydrins *ERD14* and *COR47* (Gilmour et al., 1992; Yamaguchi-Shinozaki and Shinozaki, 1993; Kiyosue et al., 1994; Nylander et al., 2001; Hoth et al., 2002; Seki et al., 2002), as well as several genes that encode signal transduction components such as the two PP2Cs, AtP2C-HA (At1g72770) and AtPP2CA (At3g11410; Rodriguez et al., 1998; Cherel et al., 2002). In addition, several transcription factors were also found in this group, including Leu zipper DNA binding proteins.

Group II contains 69 transcripts that are ABA induced in guard cells but not in mesophyll cells (Figure 5A, Table 2). Most of these genes have not been described at the cellular level. However, several have been shown to play roles in drought tolerance. For example, the trehalose-6-phosphate synthase gene is induced by ABA (Table 2) and is part of the trehalose synthase complex that functions in protection against heat and desiccation stress in microorganisms (Bell et al., 1998). In addition, overexpression of a *Saccharomyces cerevisiae* (yeast) or bacterial trehalose-6-phosphate synthase gene in *Nicotiana tabacum* (tobacco) plants was reported to lead to an increase in drought resistance (Romero et al., 1997).

Group III contains 100 transcripts that are ABA induced only in mesophyll cells (Figure 5A, see Supplemental Table 3 online). This group includes several known genes that were previously shown to be induced by ABA, such as *cor15b* (Wilhelm and Thomashow, 1993). Interestingly, several genes encoding proteins involved in sugar sensing were identified as members of this group, suggesting the existence of cross talk between sugar and ABA signaling pathways as observed in genetic analyses (reviewed in Sheen et al., 1999; Gazzarrini and McCourt, 2001).

In addition, comparison analyses with previously reported results show that among the 190 ABA-induced genes in guard cells, mesophyll cells, or both cells types, 37 genes (~20%) have been previously described to be induced in whole seedlings after 8-h treatment with 50 μM ABA: 11 only in guard cells (representing 16% of ABA-induced transcripts in guard cells), 14 only in mesophyll cells (representing 14% of ABA-induced transcripts in mesophyll cells), and 12 in both cell types (representing 52% of ABA-induced transcripts in both cell types) (Table 2, see Supplemental Table 3 online; Hoth et al., 2002). Similarly, a comparison of our results with Seki et al. (2002) revealed that 51 transcripts (~27%) of 190 genes listed in Table 2 and Supplemental Table 3 online were also reported to be induced in whole plants treated hydroponically with 100 μM ABA for 5 h: 16 only in guard cells (representing 23% of ABA-induced transcripts only in guard cells), 21 only in mesophyll cells (representing 21% of ABA-induced transcripts only in mesophyll
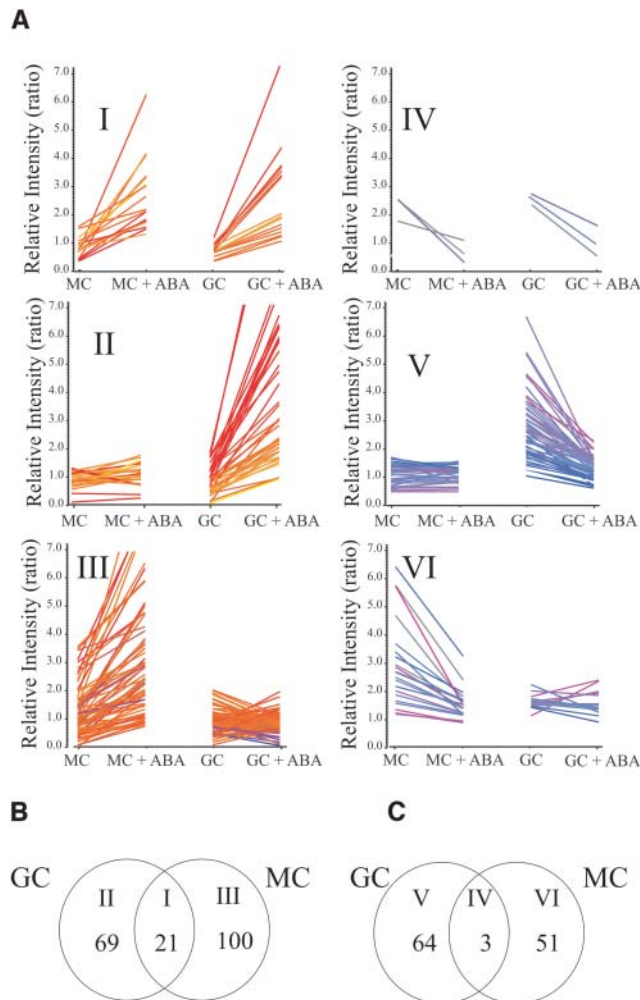
A

B   **C**

Figure 5. Cluster Analyses of Six Distinguishable ABA-Dependent Expression Responses of Guard Cell– and Mesophyll Cell–Expressed Genes.

(A) Six clusters showing distinctive ABA gene regulation patterns. Note that in the presented y axis scales, a value of 2 does not refer to a twofold increase in expression level (see Methods for log-derived values). Group I cluster contains ABA-induced genes in both guard cells and mesophyll cells. Group II cluster contains ABA-induced mRNAs only in guard cells. Group III cluster contains ABA-induced mRNAs only in mesophyll cells. Group IV cluster contains ABA-repressed mRNAs both in guard cells and mesophyll cells. Group V cluster contains ABA-repressed mRNAs only in guard cells. Group VI cluster contains ABA-repressed mRNAs only in mesophyll cells. Colors represent relative expression level of a gene after ABA treatment. Red indicates increased expression, and blue indicates reduced expression.
(B) Venn diagram presentation shows that 69 mRNAs are ABA induced only in guard cells (GC), 100 only in mesophyll cells (MC), and 21 in both cell types.
(C) Venn diagram presentation shows that 64 mRNA levels are repressed by ABA only in guard cells (GC), 51 only in mesophyll cells (MC), and three in both cell types.

cells), and 14 in both cell types (representing 67% of ABA-induced transcripts in both cell types) (Table 2, see Supplemental Table 3 online; Seki et al., 2002). Thus, many of the ABA-induced genes detected here differ from ABA-induced genes detected in whole seedlings and whole plants.

ABA-Repressed Gene Clusters

Previous studies have focused mainly on ABA upregulated transcripts. Very little knowledge exists on genes downregulated by ABA. The groups IV to VI contain transcripts that show lower expression in guard cells, mesophyll cells, or in both cell types after ABA treatment (Figures 5A and 5C). The number of genes in these three clusters is small. For example, group IV contains only three transcripts, which are slightly lower in both ABA-treated mesophyll and guard cells (Figure 5A, Table 3).

Group V contains 64 transcripts that are lower only in ABA-treated guard cells but not in mesophyll cells (Figure 5A, Table 3). Interestingly, among these genes, the *KAT1* mRNA encoding an inward potassium channel was found to be downregulated by ABA. This finding correlates with the ABA inhibition of guard cell inward K^+ channel activity that has been previously shown in guard cells from different species (Blatt and Armstrong, 1993; Lemtiri-Chlieh and MacRobbie, 1994; Schwartz et al., 1994; Lemtiri-Chlieh, 1996). In addition, of the 64 ABA-repressed transcripts in guard cells, six transcripts (∼9%) were shown to be repressed by ABA in ABA-treated whole plants (Seki et al., 2002) and only one in ABA-treated whole seedlings (Hoth et al., 2002).

Group VI contains 51 transcripts that are slightly lower in ABA-treated mesophyll cells but not in guard cells (Figure 5A, see Supplemental Table 4 online). This group includes several genes encoding proteins that function in photosynthesis, such as carbonic anhydrase, phosphoenolpyruvate carboxylase, and ribulose-1,5-bisphosphate carboxylase subunit binding protein (see Supplemental Table 4 online). The finding that ABA inhibits the expression of photosynthetic genes correlates with findings in other species (Bartholomew et al., 1991; Chang and Walling, 1991; Reinbothe et al., 1993; Weatherwax et al., 1996). In addition, ABA-repressed transcripts in mesophyll cells encode proteins that are implicated in biosynthetic functions, including amino acid and carbohydrate metabolism. Similar results have been observed in drought-stressed *Hordeum vulgare* (barley) (Ozturk et al., 2002). Of the 51 ABA-repressed transcripts in mesophyll cells (see Supplemental Table 4 online), only two transcripts were ABA-repressed in whole seedlings (Hoth et al., 2002) and in whole plants (Seki et al., 2002).

RT-PCR Confirms Microarray Data

To confirm the reliability of results from GeneChip expression profile analyses, RT-PCR experiments were performed using cDNAs synthesized from guard cell and mesophyll cell RNA. Twenty-nine genes exhibiting expression changes in response to ABA or showing differential expression in guard cells versus mesophyll cells were selected and tested two or three times. Results from eight of the tested genes are shown in Figure 6 (*CER2* [At4g24510], trehalose-6-phosphate synthase

Table 2. ABA-Induced Genes in Guard Cells

Affy Probe[a]	Description	AGI Number[b]	Cluster[c]	Experiment 1			Experiment 2			Experiment 3			Seki et al.[g]	Hoth et al.[h]
				Ratio[d]	P-Value[e]	Fold Change[f]	Ratio	P-Value	Fold Change	Ratio	P-Value	Fold Change		
12046_at	Unknown protein	At1g30690	II	1.6	0.05391	3.0	1.4	0.00031	2.6	2.1	0.00000	4.3		
12426_at	GTP binding protein	At2g21880	II	2.1	0.00001	4.3	2.8	0.00000	7.0	1.1	0.00036	2.1		
12515_at	Expansin	At2g39700	II	1.2	0.00679	2.3	1.5	0.00018	2.8	5.4	0.00000	42.2		
12521_at	Ca^{2+}/H^{+}-exchanging protein	At3g51860	II	2	0.00004	4.0	2.3	0.00108	4.9	1.3	0.00000	2.5		
12645_at	Fibrillin precursor	At4g22240	I	1.1	0.00090	2.1	1.7	0.00011	3.2	1.2	0.00000	2.3		
12749_at	Cold acclimation protein	At2g15970	I	2	0.00000	4.0	1.9	0.00000	3.7	1.4	0.00008	2.6	2.6	17.7
12753_at	Nonspecific lipid-transfer prot.	At2g38540	I	3	0.00000	8.0	2.1	0.00000	4.3	1.1	0.00000	2.1		
12754_g_at	Nonspecific lipid-transfer prot.	At2g38540	II	2.4	0.00001	5.3	4	0.00015	16.0	3.7	0.00000	13.0		
12781_at	Unknown protein	At1g13930	II	1.4	0.00000	2.6	1.7	0.00000	3.2	1.5	0.00001	2.8		
12964_at	Protease	At5g47040	II	3.2	0.00001	9.2	3.8	0.00130	13.9	1.7	0.00000	3.2		
13004_at	Senescence-associated protein	At2g17840	II	2.6	0.00053	6.1	3.5	0.00024	11.3	3	0.00000	8.0	2.63	4.1
13015_s_at	Zinc finger protein	At5g59820	II	2.6	0.00157	6.1	1.5	0.00177	2.8	1.6	0.00000	3.0	4	3.4
13067_s_at	Calcium binding protein	At1g09210	II	1.3	0.00019	2.5	1.6	0.00007	3.0	1.1	0.00002	2.1		
13084_at	Unknown protein	At1g76990	II	4.1	0.00199	17.1	1.8	0.08910	3.5	1.8	0.00012	3.5		
13128_at	PP2C	At4g31860	II	1.8	0.00000	3.5	1.8	0.00000	3.5	2.7	0.00000	6.5		
13158_at	Cinnamoyl-CoA reductase	At2g33590	I	2.3	0.00000	4.9	1.6	0.00000	3.0	2.1	0.00001	4.3	2.65	
13275_f_at	Heat shock protein	At3g46230	II	1.6	0.00061	3.0	1	0.00044	2.0	2.1	0.00065	4.3	10.71	
13279_at	Heat shock protein	At5g12020	II	4.8	0.00000	27.9	3.9	0.00001	14.9	1.2	0.00000	2.3		
13370_at	MAP kinase	At1g05100	II	3.6	0.00130	12.1	2.9	0.06494	7.5	3.1	0.00000	8.6		191
13426_at	Unknown protein	At2g41190	I	3.4	0.00009	10.6	1.9	0.00044	3.7	2.4	0.00000	5.3		28.6
13595_at	Unknown protein	At4g39730	II	1.3	0.00211	2.5	1.9	0.00022	3.7	1.8	0.00007	3.5		
13616_s_at	60S ribosomal protein	At2g39460	II	3.9	0.00000	14.9	3	0.00000	8.0	2.1	0.00000	4.3		
13617_at	Mitoch. dicarboxylate carrier	At2g22500	II	2.9	0.00177	7.5	2.0	0.34040	4.0	3.4	0.00199	10.6	1.74	
13916_at	Unknown protein	At2g19800	II	2.3	0.00000	4.9	3.3	0.00000	9.8	1.5	0.00000	2.8		
13918_at	Unknown protein	At1g54710	II	2.6	0.00715	6.1	3.2	0.00130	9.2	3.1	0.00000	8.6		5.4
13965_s_at	ABREs	At4g34000	II	3.7	0.00003	13.0	3.6	0.00008	12.1	5	0.00000	32.0		13.5
13966_at	Protein pEARLI 4	At4g35110	II	2.9	0.00014	7.5	1.5	0.00375	2.8	1.6	0.00001	3.0		
13977_at	G-3-P dehydrogenase	At2g41540	II	4.1	0.00002	17.1	1.7	0.00041	3.2	3.3	0.00000	9.8		
14052_at	Tat binding protein	At1g10070	II	2.3	0.00130	4.9	3.3	0.00003	9.8	3.7	0.00001	13.0	9.21	
14526_at	Unknown protein	At4g36210	II	2.4	0.00004	5.3	1.2	0.00074	2.3	1.6	0.00001	3.0		
14542_i_at	Putative prolylcarboxypeptidase	At2g24280	II	3.6	0.00020	12.1	1.2	0.00886	2.3	1.2	0.00002	2.3		
14666_s_at	Trehalose-6-phosphate synthase	At1g78580	II	2	0.00047	4.0	1.8	0.00000	3.5	2.5	0.00000	5.7		
14701_s_at	14-3-3 protein	At5g38480	II	1.9	0.00002	3.7	1.4	0.00001	2.6	1.7	0.00000	3.2		
14722_s_at	14-3-3 protein	At5g10450	II	1.2	0.00000	2.3	1	0.00000	2.0	1.4	0.00000	2.6		
14734_s_at	14-3-3 protein	At5g38480	II	1.7	0.00002	3.2	1.2	0.00001	2.3	1.8	0.00000	3.5		
14846_at	Calmodulin binding protein	At1g67310	II	3.8	0.00878	13.9	2.3	0.00252	4.9	3.0	0.00130	8.0		
15052_at	RD20 protein	At2g33380	I	3.8	0.00166	13.9	3.4	0.00000	10.6	1.7	0.00000	3.2	24.09	18
15053_at	DNA binding protein	At2g41870	II	2.3	0.00493	4.9	3.2	0.00267	9.2	3.5	0.00000	11.3		
15110_s_at	Dehydrin	At1g76180	I	2.1	0.00029	4.3	1.9	0.00000	3.7	1.7	0.00000	3.2		
15124_s_at	Pro oxidase	At3g30775	II	3.4	0.00000	10.6	4.9	0.00007	29.9	6.1	0.00000	68.6	6.78	
15153_at	Chlorophyll *a/b* binding protein[i]	At3g27690	II	1.7	0.00050	3.2	2	0.00022	4.0	1.2	0.00000	2.3	1.69	
15214_s_at	G-box binding transcription factor	At2g46270	II	3.7	0.00147	13.0	3.9	0.00004	14.9	3.9	0.00000	14.9	3.15	
15481_at	Unknown protein	At2g30610	II	2.7	0.00069	6.5	2	0.00005	4.0	2.2	0.00000	4.6		
15519_s_at	3-Methylcrotonyl-CoA carboxylase	At1g03090	II	3.3	0.00002	9.8	2.9	0.00000	7.5	2.3	0.00000	4.9	3.58	
15544_at	Cation transport protein	At4g31290	II	1.6	0.01183	3.0	1.8	0.00130	3.5	3.7	0.00057	13.0		3
15582_s_at	Alternative oxidase 1a precursor	At3g22370	II	2.2	0.00000	4.6	1.7	0.00000	3.2	2.1	0.00000	4.3	3.79	
15611_s_at	Low-temperature-induced protein	At5g52310	II	2.6	0.00000	6.1	3.2	0.00002	9.2	3.7	0.00000	13.0	9.09	58.3
15625_at	Glyoxalase II	At1g53580	I	2.4	0.00000	5.3	1.7	0.00000	3.2	1.6	0.00000	3.0	5.63	
15672_s_at	Arabinogalactan protein (AGP2)	At2g22470	II	2.3	0.00006	4.9	3.8	0.00000	13.9	1.9	0.00000	3.7	7.52	
15863_at	Unknown protein	At2g21820	II	2.6	0.00000	6.1	3	0.00000	8.0	2.6	0.00000	6.1		
15997_s_at	Unknown protein	At1g20440	I	2.4	0.00000	5.3	2.2	0.00000	4.6	2.7	0.00000	6.5	6.28	17
16031_at	Ferritin1 precursor	At5g01600	I	1.1	0.00147	2.1	2.1	0.00000	4.3	1.6	0.00000	3.0	2.77	
16037_s_at	Unknown protein	At1g20696	II	2.1	0.00001	4.3	1.4	0.00115	2.6	3	0.00000	8.0		
16038_s_at	Dehydrin	At5g66400	I	3.5	0.00000	11.3	3.4	0.00000	10.6	3.8	0.00000	13.9	6.83	77.6
16062_s_at	DRE CRT binding protein	At4g25470	II	2.1	0.00025	4.3	1.5	0.00096	2.8	1.8	0.00000	3.5		
16099_at	MYB family transcription factor	At4g09460	II	1.5	0.30683	2.8	2.1	0.00238	4.3	1.5	0.00000	2.8		
16115_at	Homeobox protein ATHB-12	At3g61890	I	2	0.00084	4.0	3.1	0.00002	8.6	1.1	0.00002	2.1	9.11	58
16440_at	Unknown protein	At2g40000	II	2.0	0.00549	4.0	2.7	0.00018	6.5	1.0	0.00188	2.0	3.17	
16510_at	Unknown protein	At4g32480	II	2.9	0.00079	7.5	3.6	0.00029	12.1	1.8	0.00001	3.5		
16524_at	Aldehyde dehydrogenase	At1g54100	I	1.9	0.00002	3.7	1.3	0.00001	2.5	1.5	0.00000	2.8	6.61	
16544_s_at	60S ribosomal protein	At2g39460	II	3.4	0.00000	10.6	2.9	0.00000	7.5	2.1	0.00000	4.3		
16953_at	Ribosomal protein	At1g67430	II	2.4	0.00007	5.3	2.5	0.06734	5.7	1.9	0.00000	3.7		

(Continued)

Table 2. (continued).

Affy Probe[a]	Description	AGI Number[b]	Cluster[c]	Experiment 1			Experiment 2			Experiment 3			Seki et al.[g]	Hoth et al.[h]
				Ratio[d]	P-Value[e]	Fold Change[f]	Ratio	P-Value	Fold Change	Ratio	P-Value	Fold Change		
17384_at	Unknown protein	At4g23630	II	1.0	0.00001	2.0	1.3	0.00000	2.5	1.9	0.00000	3.7		
17407_s_at	Low-temperature-induced protein	At5g52300	II	3.4	0.00098	10.6	2.7	0.00211	6.5	5.3	0.00000	39.4	12.82	
17441_s_at	Unknown protein	At1g78860	II	3.4	0.00007	10.6	2.6	0.00157	6.1	3.7	0.00000	13.0		
17442_i_at	Glycoprotein	At1g78850	II	3	0.00081	8.0	2.8	0.00022	7.0	1.7	0.00022	3.2	1.99	
17769_s_at	Trehalose-6-phosphate synthase	At1g78580	II	1.6	0.00000	3.0	1.4	0.00011	2.6	3	0.00000	8.0		
17824_s_at	MYB-related protein	At4g21440	II	5	0.00000	32.0	4.5	0.00000	22.6	2	0.00000	4.0		33
17921_s_at	Shaggy-like protein kinase	At4g18710	II	2.1	0.00252	4.3	1.6	0.13906	3.0	1.3	0.00000	2.5		
17978_s_at	MYB96 transcription factor	At5g62470	II	1.8	0.00024	3.5	1.8	0.00096	3.5	1.2	0.00000	2.3		
18594_at	Unknown protein	At1g01470	I	1.1	0.00000	2.1	1	0.00000	2.0	1.5	0.00000	2.8	4.01	4.6
18624_at	Unknown protein	At2g39570	II	4.2	0.00013	18.4	2.7	0.00267	6.5	2.9	0.00000	7.5		
18646_at	Unknown protein	At1g10590	II	1.3	0.00010	2.5	1.1	0.00004	2.1	1.3	0.00000	2.5		
18663_s_at	Unknown protein	At4g24130	II	2.2	0.00000	4.6	2.1	0.00000	4.3	1.5	0.00000	2.8		6.8
18872_at	LEA-like protein	At3g17520	II	5.4	0.00001	42.2	6.2	0.00000	73.5	5.2	0.00000	36.8		
18936_at	PP2C AtP2C-HA	At1g72770	I	4	0.00000	16.0	5.8	0.00001	55.7	2.2	0.00000	4.6		3.5
18949_at	MYB-related protein	At5g67300	II	5.1	0.00000	34.3	1.6	0.00065	3.0	2.2	0.00000	4.6		
18955_at	β-Ketoacyl-CoA synthase	At1g04220	II	1.6	0.01183	3.0	2.5	0.00299	5.7	2.1	0.00000	4.3		3.2
19152_at	LEA	At5g06760	I	3.5	0.00000	11.3	6.6	0.00000	97.0	3.4	0.00000	10.6	13.29	328
19186_s_at	Dehydrin Xero2	At3g50970	I	2.9	0.00000	7.5	3.1	0.00000	8.6	4.5	0.00000	22.6		
19441_s_at	G-box binding factor	At4g01120	II	4.3	0.00139	19.7	1.7	0.00012	3.2	3	0.00004	8.0		
19638_at	PP2C	At3g11410	I	3.6	0.00000	12.1	2.1	0.00000	4.3	2.9	0.00000	7.5	7.58	4.6
19646_at	Homeodomain transcription factor	At2g46680	I	3.9	0.00000	14.9	3.4	0.00000	10.6	2.3	0.00000	4.9	8.84	27.7
19688_at	Low-temperature-induced protein	At4g25580	II	1.0	0.01897	2.0	3.5	0.00166	11.3	2.6	0.00000	6.1		
19852_s_at	Cytoplasmatic aconitate hydratase	At4g35830	II	1.1	0.00003	2.1	1.1	0.00001	2.1	1.8	0.00000	3.5		
19860_at	Transcription factor	At1g56170	II	1.6	0.00038	3.0	1.4	0.00130	2.6	1.8	0.00000	3.5		4
19982_at	Unknown protein	At1g79270	I	3.5	0.00753	11.3	1.3	0.00044	2.5	3.8	0.00000	13.9		
20042_at	No hits		II	2.7	0.00000	6.5	2.4	0.00000	5.3	1.3	0.00000	2.5		
20060_at	No hits		II	5	0.00001	32.0	2.8	0.00006	7.0	2.3	0.00000	4.9		
20186_at	Unknown protein	At1g08630	II	2.3	0.00299	4.9	1.1	0.00009	2.1	2.1	0.00001	4.3		
20200_at	Unknown protein	At4g25690	II	1.4	0.02480	2.6	1.2	0.00029	2.3	1.3	0.00000	2.5	1.89	
20323_at	Small heat shock protein	At2g29500	II	3.4	0.00018	10.6	1.2	0.00027	2.3	2.1	0.00001	4.3		
20635_s_at	MYB96 transcription factor	At5g62470	II	1.0	0.02705	2.0	2.2	0.00019	4.6	1.1	0.00000	2.1		
20641_at	LEA	At1g52690	I	4.9	0.00001	29.9	6.6	0.00000	97.0	3.6	0.00000	12.1	30.75	1799

[a] Describes names of probe set on Affymetrix chip.

[b] AGI locus numbers.

[c] Indicates clusters in Figure 5.

[d] Signal log value, which measures the change in expression level for a transcript between two arrays. This change is expressed as the $\log_2$ ratio. A $\log_2$ ratio of 1 is the same as a fold change of 2.

[e] Change P-value, which measures the probability that the expression levels of a probe in two different arrays are the same. Change P-values of 0.00000 correspond to P-value <0.000005.

[f] Fold change is calculated using the signal log ratio (see Methods).

[g] Obtained from Supplemental Table 1 online (column for 5-h ABA treatment; Seki et al., 2002).

[h] Obtained from Supplemental Table Induced.xls online (Hoth et al., 2002).

[i] Chlorophyll *a/b* binding protein gene expression is repressed by ABA at 1, 2, 10, and 24 h of ABA treatment but shows ABA induction at 5 h of ABA treatment (see Seki et al., 2002, Supplemental Table 5 online).

[At1g78580], *LEA* [At5g06760], *KAT1* [At5g46240], CDPK [At3g51850], dehydrin [At3g50970], PP2C [At3g11410], and *COR47* [At1g20440]). All of the analyzed genes exhibited cell type specificity or ABA regulation in RT-PCR experiments that correlated with our GeneChip results (see Supplemental Figure 2 online), indicating reliability of the microarray data.

Promoter Element Analyses

To analyze ABA-regulated promoter sequences, statistical analyses of *cis*-acting elements were pursued. Functional analyses

and sequence comparison of ABA-inducible promoters allowed the identification of *cis*-acting sequences, such as the G-box–containing elements designated ABA-regulated elements (ABREs) and the functionally equivalent coupling element3 (CE3)–like sequences (reviewed in Busk and Pages, 1998). Our gene expression results allow us to statistically explore the correlation between these elements and ABA regulation on a global scale and to test the generality of hypotheses generated from the few experimentally analyzed promoters in different plant species. Table 4 shows results from our analysis

Table 3. ABA-Repressed Genes in Guard Cells

Affy Probe[a]	Description	AGI Number[b]	Cluster[c]	Experiment 1			Experiment 2			Experiment 3			Seki et al.[g]	Hoth et al.[h]
				Ratio[d]	P-Value[e]	Fold Change[f]	Ratio	P-Value	Fold Change	Ratio	P-Value	Fold Change		
12100_at	MYB family transcription factor	At2g21650	V	−3.8	0.99997	−13.9	−3.3	0.99999	−9.8	−3.4	0.99997	−10.6		
12185_at	Unknown protein	At1g54860	V	−1.8	0.95007	−3.5	−2.1	0.99898	−4.3	−1.7	0.99733	−3.25		
12196_at	Unknown protein	At2g28410	V	−1.5	1.00000	−2.8	−1.8	1.00000	−3.5	−2	0.99998	−4.0		
12284_at	Somatic embryogenesis receptor kinase	At1g34210	V	−0.8	0.96060	−2	−1.4	0.99977	−2.6	−2	0.99980	−4.0		4.7
12338_at	Pectin methylesterase	At3g14310	V	−4.1	0.99994	−17.1	−1.7	0.99977	−3.2	−2.3	0.97409	−4.9		
12381_at	No hits		V	−0.6	0.94811	−2	−0.7	0.99733	−2	−1.5	0.99996	−2.8		
12409_at	Small nuclear ribonucleoprotein U1A	At2g47580	V	−0.8	1.00000	−2	−0.9	0.99992	−2	−2.4	1.00000	−5.3		
12768_at	Unknown protein	At2g15890	V	−0.9	0.99999	−2	−0.7	0.99995	−2	−1.6	0.99973	−3.0		
12773_at	Membrane channel protein	At2g28900	V	−0.9	1.00000	−2	−0.6	1.00000	−2	−1.2	0.99122	−2.3		
12843_s_at	Unknown protein	At2g16590	V	−1.0	0.99994	−2	−0.6	0.99947	−2	−0.8	0.50000	−2		
12846_s_at	No hits		V	−2.1	1.00000	−4.3	−0.8	0.99999	−2.0	−1.5	1.00000	−2.8		
12881_s_at	No hits		V	−1.6	0.99995	−3.0	−0.7	1.00000	−2	−2.3	1.00000	−4.9		
12893_at	Alcohol dehydrogenase	At5g43940	V	−1.6	0.99989	−3.0	−0.6	0.99964	−2	−1.6	0.99998	−3.0		
13080_at	40S ribosomal protein	At2g21580	V	−0.7	0.99776	−2	−0.6	0.99905	−2	−1.8	1.00000	−3.5		
13184_s_at	Thioredoxin	At5g42980	V	−2.3	1.00000	−4.9	−0.6	1.00000	−2.0	−0.9	0.86906	−2		
13236_at	Aldolase	At4g39980	V	−0.6	0.97627	−2	−1.2	0.99843	−2.3	−2.1	1.00000	−4.3		
13254_at	Farnesyl pyrophosphate synthetase2	At4g17190	V	−0.7	0.99999	−2	−0.7	0.99973	−2	−1.8	1.00000	−3.5		
13554_at	β-Ketoacyl-CoA synthase	At2g16280	V	−1.1	0.99853	−2.1	−1.6	1.00000	−3.0	−1.8	0.99776	−3.5		
13672_at	No hits		V	−0.9	0.99967	−2	−1	0.99993	−2	−1.4	0.99939	−2.6		
14090_i_at	Unknown protein	At2g15830	V	−0.6	0.99820	−2	−0.6	1.00000	−2	−0.7	0.76103	−2		
14663_s_at	Glycosyl hydrolase family	At4g24040	V	−1.0	0.99978	−2	−0.6	0.99910	−2	−0.6	0.49254	−2		
14667_at	TRP synthase	At5g54810	V	−0.7	0.99977	−2	−0.9	0.99967	−2	−2.3	0.99999	−4.9		
14717_s_at	CLC-a chloride channel protein	At5g40890	V	−0.7	0.99993	−2	−1.1	1.00000	−2.1	−2.6	1.00000	−6.1		
15105_s_at	Gly-rich RNA binding protein	At2g21660	V	−1.1	0.99992	−2.1	−1.3	1.00000	−2.5	0.2	0.00000	−2	0.8	
15194_s_at	GASA4	At5g15230	IV	−0.8	1.00000	−2	−0.9	1.00000	−2	−0.8	0.89823	−2		
15213_s_at	Orn carbamoyltransferase	At1g75330	V	−0.8	0.99991	−2	−0.9	1.00000	−2	−2	1.00000	−4.0		
15453_at	Unknown protein	At4g14020	V	−0.9	0.99999	−2	−0.7	0.99990	−2	−1.9	1.00000	−3.7		
15510_r_at	No hits		V	−1.8	0.82023	−3.5	−0.8	0.99989	−2	−2.1	1.00000	−4.3		
15548_at	Unknown protein	At1g11820	V	−0.9	0.99971	−2	−0.7	0.99978	−2	−2.3	1.00000	−4.9		
15624_s_at	ADPG pyrophosphorylase	At5g48300	IV	−0.6	0.99931	−2	−1.2	1.00000	−2.3	−2.2	1.00000	−4.6		
15626_s_at	Vacuolar sorting receptor	At3g52850	V	−0.6	0.98817	−2	−0.8	0.99998	−2	−1.7	0.99999	−3.2		
15703_i_at	Putative trypsin inhibitor	At2g43520	V	−2.6	0.99971	−6.1	−0.8	1.00000	−2.0	−1.8	0.99934	−3.5		
16014_at	Unknown protein	At1g75750	V	−0.8	1.00000	−2	−0.8	1.00000	−2	−1.9	0.99999	−3.7		
16042_s_at	Cytochrome P450[i]	At5g05690	V	−0.7	0.99910	−2	−1.3	0.99986	−2.5	−0.7	0.54467	−2	1.2	
16051_at	Tubulin β-9 chain	At4g20890	V	−1.2	0.99997	−2.3	−0.9	0.99988	−2	−1.6	0.99990	−3.0		
16092_s_at	Potassium channel protein KAT1	At5g46240	V	−2.3	0.99981	−4.9	−1.5	0.99999	−2.8	−2.3	0.99999	−4.9		
16118_s_at	WD-40 repeat protein	At2g19520	V	−0.7	0.50000	−2	−0.9	0.99905	−2	−2.5	1.00000	−5.7		
16145_at	Vacuolar ATP synthase	At1g75630	V	−1.0	1.00000	−2.0	−0.9	0.99996	−2	−2.9	0.99999	−7.5		
16416_at	Plant defensin protein	At2g02130	V	−0.8	0.99989	−2	−1.8	1.00000	−3.5	−0.9	0.92765	−2		
16430_at	Glutathione S-transferase[j]	At2g30860	V	−0.8	0.99733	−2	−1.3	1.00000	−2.5	−2	1.00000	−4.0	1.1	
16451_at	Ketol-acid reductoisomerase	At3g58610	V	−1.3	0.99420	−2.5	−1.5	1.00000	−2.8	−1.6	0.99999	−3.0		
16458_s_at	No hits		V	−0.9	0.99993	−2	−0.7	0.99980	−2	−1.6	0.70618	−3.0		
16624_s_at	Transcription factor	At1g08810	V	−0.6	0.84813	−2	−1.4	1.00000	−2.6	−1.9	0.99997	−3.7		
16897_i_at	Unknown protein	At5g15350	V	−0.7	0.99713	−2	−1	0.99992	−2	−2.3	0.99994	−4.9		
16985_s_at	Cytosolic ribosomal protein	At3g48930	V	−0.7	1.00000	−2	−0.6	0.99999	−2	−1.9	0.99994	−3.7		
16998_at	dTDP-glucose 4-6-dehydratase	At3g62830	V	−0.7	0.99962	−2	−0.6	0.99985	−2	−1.8	0.99998	−3.5		
17033_at	Unknown protein	At5g39410	V	−1.0	0.99910	−2.0	−1	0.99999	−2.0	−1.4	0.90472	−2.64		
17126_at	WD-40 repeat protein	At5g58230	V	−0.9	0.82023	−2	−0.6	0.99992	−2	−2.1	1.00000	−4.3		
17187_at	Putative arginase	At4g08870	V	−3.2	0.99853	−9.2	−1.6	0.99763	−3.0	−1.4	0.99479	−2.64		
17215_at	Trypsin inhibitor	At2g43550	V	−0.8	0.94609	−2	−1	0.99950	−2	−2.1	0.99991	−4.3		
17237_at	Unknown protein	At2g22840	V	−1.7	0.77836	−3.2	−2.3	0.99926	−4.9	−2.6	0.99973	−6.06		
17865_at	NADPH oxidoreductase	At1g75280	V	−1.2	0.97295	−2.3	−2.7	0.99939	−6.5	−1.8	0.99984	−3.48		
17957_at	Acetone-cyanohydrin lyase	At2g23600	IV	−1.2	0.99910	−2.3	−3.3	1.00000	−9.8	−2.9	1.00000	−7.46		
18063_i_at	No hits		V	−1.2	0.99425	−2.3	−1	0.99915	−2.0	−2.7	0.99997	−6.5		
18272_at	Unknown protein	At2g40080	V	−1.1	0.94402	−2.1	−3.9	1.00000	−14.9	−2.7	0.99999	−6.5		

(Continued)

Table 3. (continued).

Affy Probe[a]	Description	AGI Number[b]	Cluster[c]	Experiment 1			Experiment 2			Experiment 3			Seki et al.[g]	Hoth et al.[h]
				Ratio[d]	P-Value[e]	Fold Change[f]	Ratio	P-Value	Fold Change	Ratio	P-Value	Fold Change		
18315_s_at	β-Glucosidase	At4g27830	V	−0.7	0.99718	−2	−1.1	0.98873	−2.1	−2.3	0.99999	−4.9		
18611_at	Putative pyruvate water dikinase	At5g26570	V	−1.1	0.99823	−2.1	−0.7	0.99843	−2	0.4	0.31342	−2		
18678_at	Peptidylprolyl isomerase ROC4	At3g62030	V	−1.8	0.99853	−3.5	−0.9	0.99995	−2	−2.5	1.00000	−5.7	0.19	
18687_at	Pyruvate dehydrogenase subunit	At1g59900	V	−0.7	0.99973	−2	−0.8	1.00000	−2	−1.8	1.00000	−3.5		
18708_at	Ripening-related protein	At5g62350	V	−1.4	0.99998	−2.6	−2.3	1.00000	−4.9	−2.8	1.00000	−7.0	0.66	
18882_at	No hits		V	−0.7	0.99996	−2	−0.7	0.99943	−2	−1.8	1.00000	−3.5		
18956_at	Ethylene response sensor	At2g40940	V	−0.7	0.99943	−2	−0.6	0.99992	−2	−1.9	1.00000	−3.7		
19171_at	Trypsin inhibitor[k]	At2g43510	V	−1.5	0.99967	−2.8	−0.6	0.99885	−2	−2.5	1.00000	−5.7	2.97	
20282_at	Protein kinase	At2g28930	V	−1.3	0.99989	−2.5	−1.3	1.00000	−2.5	−3.2	1.00000	−9.2		
20537_at	Extensin	At4g13340	V	−1.6	0.99892	−3.0	−0.9	0.99733	−2	−1.2	0.93019	−2.3		
20585_at	Glutaredoxin	At2g47880	V	−1.7	0.99994	−3.2	−1.9	0.94811	−3.7	−1.6	0.99950	−3.03		
20709_s_at	Putative 3-oxoacyl reductase	At1g24360	V	−0.6	0.99998	−2	−0.6	0.99998	−2	−2.2	1.00000	−4.6		

[a] Describes names of probe set on Affymetrix chip.

[b] AGI locus numbers.

[c] Indicates clusters in Figure 5.

[d] Signal Log value which measures the change in expression level for a transcript between two arrays. This change is expressed as the $\log_2$ ratio. A $\log_2$ ratio of 1 is the same as a Fold change of 2.

[e] Change P-value, which measures the probability that the expression levels of a probe in two different arrays are the same. Change P-values of 1.00000 correspond to P-value >0.99995.

[f] Fold change is calculated using the signal log ratio.

[g] Obtained from Supplemental Table 5 online (column for 5-h ABA treatment; Seki et al., 2002).

[h] Obtained from Supplemental Table Repressed.xls online (Hoth et al., 2002).

[i] Cytochrome p450 gene expression is repressed by ABA at 1, 2, 10, and 24 h of ABA treatment but shows ABA induction at 5 h of ABA treatment.

[j] GST gene expression is slightly induced by ABA at 1, 5, and 10 h of ABA treatment but repressed by ABA at 2 and 24 h of ABA treatment (see Seki et al., 2002, Supplemental Table 5 online).

[k] Trypsin inhibitor gene is induced by ABA (see Seki et al., 2002, Supplemental Table 1 online).

of the occurrence of several known ABA-related *cis*-regulatory motifs in the 500-bp upstream sequences. Pattern match searches were performed by writing custom Python scripts with C extensions (see Methods). The number and percentage of occurrences (hits) of each motif are given for each gene set (Table 4, columns A to E). To evaluate the significance of these numbers and percentages, a P-value was computed giving the probability of obtaining at least as many hits as were observed in the set, if the set were a random sample drawn without replacement from the complete set of Arabidopsis promoter sequences. A small P-value for a given motif and set shows that the observed number of hits is unlikely to be because of chance (Table 4). In further controls, ABA-repressed transcripts were also analyzed, and the analyzed motifs were found not to be significantly overrepresented (Table 4, columns B and D).

Our analyses showed that the classical G-box containing ABRE is significantly overrepresented in the set of ABA-induced genes in both guard cells ($P < 10^{-13}$) and mesophyll cells ($P < 10^{-7}$) (Table 4, row 2, columns C and E). Moreover, its occurrence in non-ABA-induced gene sets is not more than would be expected by chance (Table 4, rows 1 and 2, columns B and D; data not shown). This result statistically confirms that the classical ABRE is a predictor of ABA induction. A sequence (ACGCGTGTC) was computationally derived with similarity to the coupling element CE3 from *H. vulgare*. This sequence is also mildly overrepresented in the ABA-induced gene sets (Table 4, row 6, column C). The dehydration-responsive element (DRE), which has been reported in the promoter regions of drought- and cold-inducible genes, is also statistically overrepresented in the ABA-induced genes in mesophyll cells but not in guard cells (Table 4, rows 7 and 8, columns C and E).

In addition to searching for known motifs, we applied the motif-finding program AlignACE 3.0 that uses a Gibbs sampling algorithm (http://atlas.med.harvard.edu/; Hughes et al., 2000) to each of the promoter sequence sets. AlignACE found a strong signal for an ABRE-like motif with the consensus sequence (C/G)ACGTG(G/T)(A/C) in both sets of ABA-induced genes (Table 4, row 1) but not in the non-ABA-induced gene sets. This pattern represents a subset of the classical G-box containing ABRE (C/G/T)ACGTG(G/T)(A/C) (Shinozaki and Yamaguchi-Shinozaki, 2000).

Expression Profiling of ABA Signaling Components in Guard Cells

Expression profiling has been proposed as a method to produce new hypotheses for possible roles of genes and proteins in signal
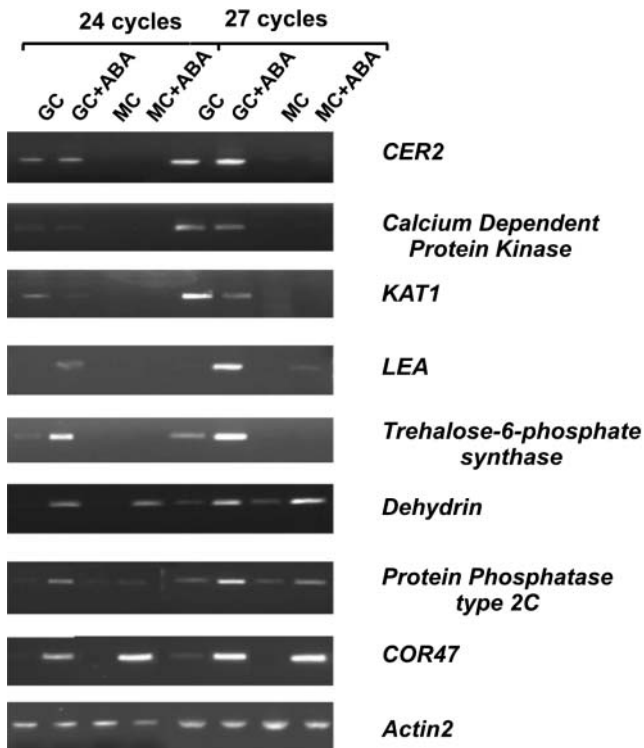
Figure 6. RT-PCR Analyses Independently Confirm Results Obtained from Chip Hybridization Experiments.

RT-PCR was performed using guard cell and mesophyll cell RNA with primers for selected genes from guard cell preferential genes showing no ABA modulation (*CER2* and calcium-dependent protein kinase [At3g50530]) and from Figure 5–derived group I (dehydrin [At3g50970], PP2C [At3g11410], and *COR47*), group II (trehalose-6-phosphate synthase and *LEA*) and group V (*KAT1*). Results are from 24 and 27 RT-PCR cycles. *Actin2* gene was used as control. Results from 8 of 29 tested genes are illustrated. PCR was repeated at least twice. GC; guard cells; GC + ABA, guard cells treated with ABA; MC, mesophyll cells; MC + ABA, mesophyll cells treated with ABA.

transduction (Hughes et al., 2000; Perez-Amador et al., 2001). To test this hypothesis, we investigated the genes that were described previously to function in early ABA signaling in guard cells and that were present on the chip. To test whether transcript levels of these genes are modulated, we analyzed their regulation by ABA. A simplified model including previously demonstrated positive transducers and negative regulators mediating guard cell ABA signal transduction is shown in Figure 7 (Cutler et al., 1996; Leung et al., 1997; Pei et al., 1997, 1998, 2000; Allen et al., 2001, 2002; Hugouvieux et al., 2001; Murata et al., 2001; Cherel et al., 2002; Kwak et al., 2002, 2003; Mustilli et al., 2002; Yoshida et al., 2002). This figure is color coded to show the relative expression of the components before and after ABA treatment. Interestingly, many mRNAs of genes known to function in ABA signal transduction (see Mäser et al., 2003) were regulated by ABA in guard cells (Figure 7). For example, the two PP2C genes, *ABI1* and *ABI2*, are induced by ABA in both guard cells and

mesophyll cells. Interestingly, *ABH1* and the dominant *abi1-1* and *abi2-1* alleles are negative regulators of ABA signaling, and their mRNA levels are increased by ABA, whereas the transcript level of another negative regulator *ERA1* is reduced by ABA.

K$^+$ uptake channels, which contribute to K$^+$ uptake during stomatal opening, are negative effectors of ABA-induced ion efflux. The K$^+$ uptake channel transcripts such as *KAT1*, *KAT2*, and *AKT2* are repressed by ABA. Moreover, *AtPP2CA*, which has been shown to inhibit the AKT2 inward-rectifying K$^+$ channel activity in heterologous systems (Cherel et al., 2002), is induced by ABA.

From Single Cell Expression Profiling to Gene Function: Identification of a PP2C That Functions in ABA Signaling

To verify that the microarray approach to functional discovery is effective, we selected one PP2C gene, *AtP2C-HA*, because it is a PP2C transcript that showed a very high level of ABA upregulation in guard cells and because no recessive knockout mutant phenotypes of PP2Cs have yet been reported in plants. *AtP2C-HA* was identified previously as an ABA-induced transcript with homology to *ABI1* and *ABI2* (Rodriguez et al., 1998).

We identified an *atp2C-HA-1* disruption mutant carrying a single T-DNA insertion from the SALK Institute Genomic Analysis Laboratory (SIGnAL) database of sequenced T-DNA mutagenized Arabidopsis lines. The T-DNA insertion was in the third intron of *AtP2C-HA* (Figure 8A). RNA gel blot analysis confirmed the ABA induction of *AtP2C-HA* mRNA in the wild type, which was abolished in homozygous *atp2C-HA-1* plants (Figure 8B). To determine whether the *atp2C-HA-1* disruption mutation affects stomatal responses to ABA, we performed ABA-induced stomatal closing assays. Figure 8C shows that ABA-induced stomatal closing in *atp2C-HA-1* mutant plants was more sensitive to ABA than that in the wild type at 0.01 μM ABA. In addition, we examined whether *AtP2C-HA* may also function in ABA-mediated inhibition of seed germination. Interestingly, the loss of *AtP2C-HA* function confers a substantial ABA-hypersensitive regulation of seed germination under the conditions assayed (Figure 8D). ABA hypersensitivity showed a 1:3 segregation in backcrossed F2 lines, indicating that *atp2C-HA-1* is a recessive mutant. To test whether the ABA-hypersensitive phenotype of *atp2C-HA-1* is the result of *AtP2C-HA* gene disruption, we tested complementation of the *atp2C-HA-1* mutant with the *At2PC-HA* cDNA, which restored *At2PC-HA* expression (Figure 8E). Two independent complemented *atp2C-HA-1* lines showed wild-type responses in both ABA-induced stomatal closing assays (Figure 8C) and ABA inhibition of seed germination assays (Figure 8D). These results suggest that AtP2C-HA functions as a negative regulator of ABA signal transduction and illustrate that the combination of guard cell expression data and functional genomic approaches can be used to identify gene function.

DISCUSSION

This study reports cell type–specific characterization of gene expression patterns in guard cells and mesophyll cells and their

Table 4. Occurrence of Motifs in 500-bp Region Upstream of ABA-Regulated Genes

Motif	Sequence	Allowed Mismatches	Reference	A All Sequences			B Guard Cell, ABA Downregulated				C Guard Cell, ABA Upregulated				D Mesophyll Cell, ABA Downregulated				E Mesophyll Cell, ABA Upregulated			
				Hits	Set Size	Pct	Hits	Set Size	Pct	P-Value	Hits	Set Size	Pct	P-Value	Hits	Set Size	Pct	P-Value	Hits	Set Size	Pct	P-Value
1 ABRE from AlignACE	(C/G)ACGTG-(G/T)(A/C)	0	This article	831	7749	11	3	59	5.1	9.60E−01	34	92	37	**2.26E−11**	6	53	11	5.09E−01	33	120	28	**2.07E−07**
2 Classical ABRE	(C/G/T)ACGTG-(G/T)(A/C)	0	Ref 1	1121	7749	14	4	59	6.8	9.79E−01	43	92	47	**9.78E−14**	10	53	19	2.29E−01	42	120	35	**1.21E−08**
3 CE1	TGCCACCGG	0	Ref 2	3	7749	0.0	0	59	0.0	1.00E+00	0	92	0.0	1.00E+00	0	53	0.0	1.00E+00	0	120	0.0	1.00E+00
4 CE1	TGCCACCGG	1	Ref 2	135	7749	2.0	2	59	3.4	2.75E−01	2	92	2.2	4.79E−01	3	53	5.7	6.45E−02	3	120	2.5	3.48E−01
5 CE3, Full	ACGCGTGTCCTC	1	Ref 2	14	7749	0.0	0	59	0.0	1.00E+00	1	92	1.1	1.54E−01	0	53	0.0	1.00E+00	0	120	0.0	1.00E+00
6 CE3, Short	ACGCGTGTC	0	This article	11	7749	0.0	0	59	0.0	1.00E+00	2	92	2.2	**7.15E−03**	0	53	0.0	1.00E+00	0	120	0.0	1.00E+00
7 DRE	TACCGACAT	0	Ref 2	14	7749	0.0	0	59	0.0	1.00E+00	2	92	2.2	1.16E−02	0	53	0.0	1.00E+00	4	120	3.3	**4.86E−05**
8 DRE	TACCGACAT	1	Ref 2	364	7749	5.0	1	59	1.7	9.42E−01	8	92	8.7	6.67E−02	5	53	9.4	1.02E−02	14	120	12	**1.42E−03**

For each motif, the number (Hits) and percentage (Pct) of promoters in each gene set containing at least one occurrence of the given motif are shown. Occurrence of the motifs was determined by scanning for either exact (Allowed Mismatches = 0) or inexact (Allowed Mismatches = 1) pattern matches on both strands of the 500 nucleotides upstream of the translational start. Significantly overrepresented motifs have P-values ≤0.01, which are in bold. Ref 1, Shinozaki and Yamaguchi-Shinozaki (2000); Ref 2, Busk and Pages (1998).

regulation by ABA. For most of the genes studied here, no previously published data have been available with respect to their expression in guard cells and mesophyll cells. These data provide initial information, which could lead to characterization of gene functions in these cell types. For example, the identification of two ABA-induced guard cell preferential genes encoding trehalose synthase complex proteins can direct future analysis of the phenotype of mutants or transgenic plants altered in the expression of these genes. Moreover, a large number of the guard cell–expressed genes have unknown functions, and, therefore, the tools and signal transduction branches characterized in guard cells can guide future work in functional genomic, cell biological, biophysical, and biochemical characterizations. Analyses of expression data show differences in guard cell and mesophyll cell expression profiles (Figures 5 and 6, Table 1, see Supplemental Tables 1 and 2 online). Importantly, the results indicate that a relatively small fraction of genes are expressed in a strictly cell type–specific manner. Note, however, that the relative expression level of a given gene or protein is an additional important factor and can differ among cell types. This finding supports a model in which combinatorial and temporal permutation in gene expression profiles and transcript processing are important for achieving specialized functions of cells, a model that is also being strongly considered for other organisms, in which relatively small genomes give rise to a high level of sophistication (e.g., The International Human Genome Mapping Consortium, 2001).

Identification of New ABA-Regulated Genes

Only a few ABA-regulated genes had been reported until recently. The present guard cell expression study and recently reported analyses of mRNA extracted from whole seedlings or whole plants (Seki et al., 2001, 2002; Hoth et al., 2002) show that the mRNA levels of many genes are ABA regulated, providing additional marker genes for mutant analyses. Interestingly, the presented data also show differences in ABA regulation of gene expression in these different studies (Tables 2 and 3, see

Supplemental Tables 2 and 3 online). This is likely because of the differences in methods used, including differences in plant materials (whole plants versus guard cells), differences in the methods for growing plants and ABA treatments, and differences in microarray technologies (full-length cDNA versus computationally selected oligonucleotide probes). Our results, therefore, together with Seki et al. (2002) and Hoth et al. (2002), provide diverse resources of ABA-regulated genes with different spectrums in genes identified from microarray experiments.

On the basis of microarray and RT-PCR analyses presented here, we found 190 ABA-induced genes and 118 ABA-repressed genes, which have been grouped according to cell type expression (Figure 5). Among ABA-induced genes, 69 were induced preferentially in guard cells (Figures 5A and 5B, Table 2), 100 in mesophyll cells (Figures 5A and 5B, see Supplemental Table 3 online), and 21 in both cell types (Figures 5A and 5B, Table 2, see Supplemental Table 3 online). Differences in ABA-induced genes in guard cells and mesophyll cells may in part be the result of differential accessibility of these cells to exogenous ABA.

The ABA upregulated genes reported here can be classified in two major classes with respect to their putative functions: (1) genes implicated in cell protection and in the production of important metabolic proteins and (2) genes implicated in signal transduction. The first class includes proteins that probably function in stress tolerance, such as enzymes required for the biosynthesis of osmoprotectants (sugars) and proteins that may protect macromolecules and membranes (LEA and Chaperones). The second class contains proteins that may function in signal transduction and stress tolerance, such as protein kinases, protein phosphatases, receptor kinases, transcription factors, 14-3-3 proteins, reactive oxygen turnover enzymes (NADPH oxidases, catalase, and glutathione S-transferase), and protein turnover mechanisms (ubiquitination). The identification and characterization of these putative regulatory proteins will contribute to further analyses of the ABA signaling network in plants. Moreover, the study of uncharacterized transcription factors, which are highly induced in response to ABA, may provide clues toward further characterizing a transcriptional
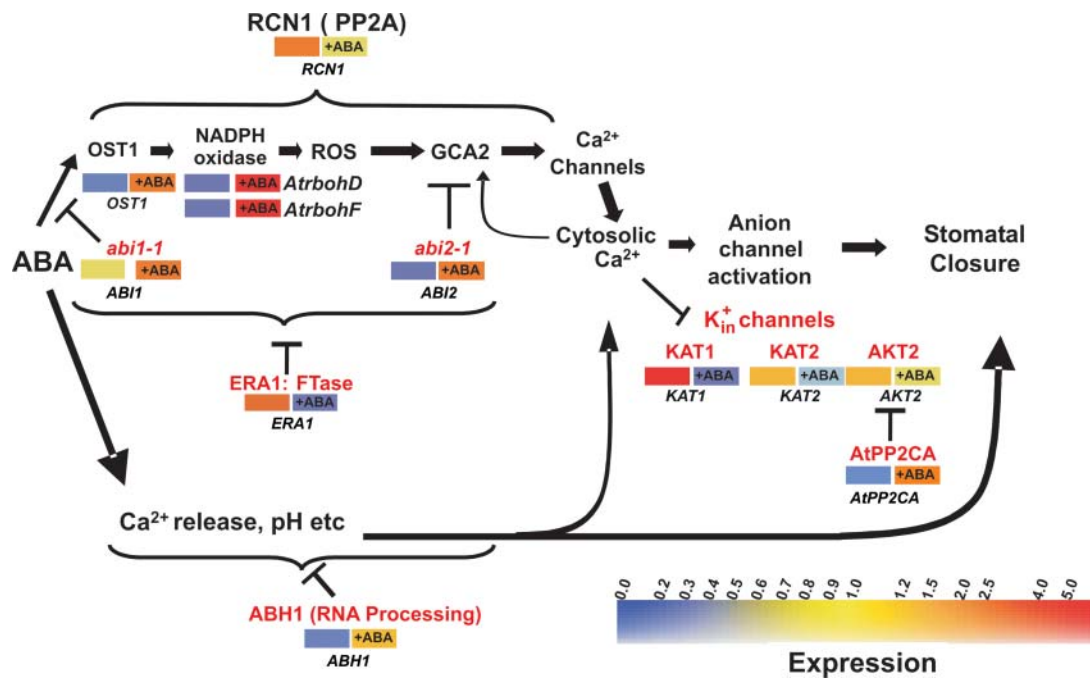
Figure 7. Schematic Representation of ABA-Regulated Guard Cell–Expressed Genes in Current Working Model for ABA Signal Transduction Shows That the Transcript Levels of ABA Signal Transducers Are Regulated by ABA in Guard Cells.

Negative regulators and effectors are shown in red for clarity. Colors in boxes represent relative expression level of a gene before and after ABA treatment (+ABA). Low message level genes are included for this model, and genes not present on the chip are excluded in the model.

control network of genes that mediate physiological ABA responses.

In addition, we show here that the transcripts of 118 genes are repressed by ABA; 64 of these are preferentially ABA repressed in guard cells (Figures 5A and 5C, Table 3), 51 in mesophyll cells (Figures 5A and 5C, see Supplemental Table 4 online), and three in both cell types (Figures 5A and 5C, Table 3, see Supplemental Table 4 online). Until now, mainly photosynthesis-related genes have been characterized as repressed by ABA (Weatherwax et al., 1996), but our data show that several genes that function in signal transduction and osmoregulation, such as protein kinases and the K$^+$ channels *KAT1*, *KAT2*, and *AKT2*, are also repressed by ABA.

Statistical Analysis of ABA-Responsive *cis*-Elements

Several *cis*-regulatory elements have been shown previously to contribute to ABA responses of individual genes such as the G-box–containing ABREs, the coupling elements CE1 and CE3, the RY/Sph elements, and the recognition sequences for the MYB and MYC class of transcription factors (reviewed in Busk and Pages, 1998). In this study, analysis of the promoter regions of ABA-induced genes shows that promoters containing one or more copies of an ABRE-like motif, (C/T)ACGTG(G/T)(A/T), and a motif similar to the *H. vulgare* coupling element CE3 are significantly overrepresented in the set of ABA induced genes (Table 4, row 1). Interestingly, ABRE-like elements are not found for all ABA-induced genes, and the large number of new ABA-induced or -repressed genes described in this study provides

a basis for combinatorial analyses of different elements and a better understanding of the contribution of new *cis*-acting elements to ABA-dependent gene expression and cell type specificity.

ABA Modulation of Guard Cell ABA Signal Transduction Components

To date, relatively few genes acting in ABA signaling have been identified using genetic screens based on whole-plant or whole-tissue phenotypes (see Introduction). The guard cell system has been adapted and developed to dissect where and how ABA signaling mechanisms function within the network. Unexpectedly, we have found that all of the known ABA signal transducers and negative regulators of ABA signaling represented on the GeneChip are ABA modulated at the transcript level in guard cells (Figure 7). These findings suggest the existence of feedback regulation or parallel ABA regulation of transcript levels, which may occur via transcription and mRNA processing. Recent studies suggest the importance of RNA processing in ABA signal transduction (Lu and Fedoroff, 2000; Hugouvieux et al., 2001; Xiong et al., 2001a; Li et al., 2002). These data indicate that modulation of mRNA levels may be of broad general importance for early ABA signal transduction. Therefore, ABA-mediated expression profiling provides an approach for selection of putative signal transducers that are members of large gene families (Figure 8) or are genes presently of unknown function for biochemical and cell biological analyses.
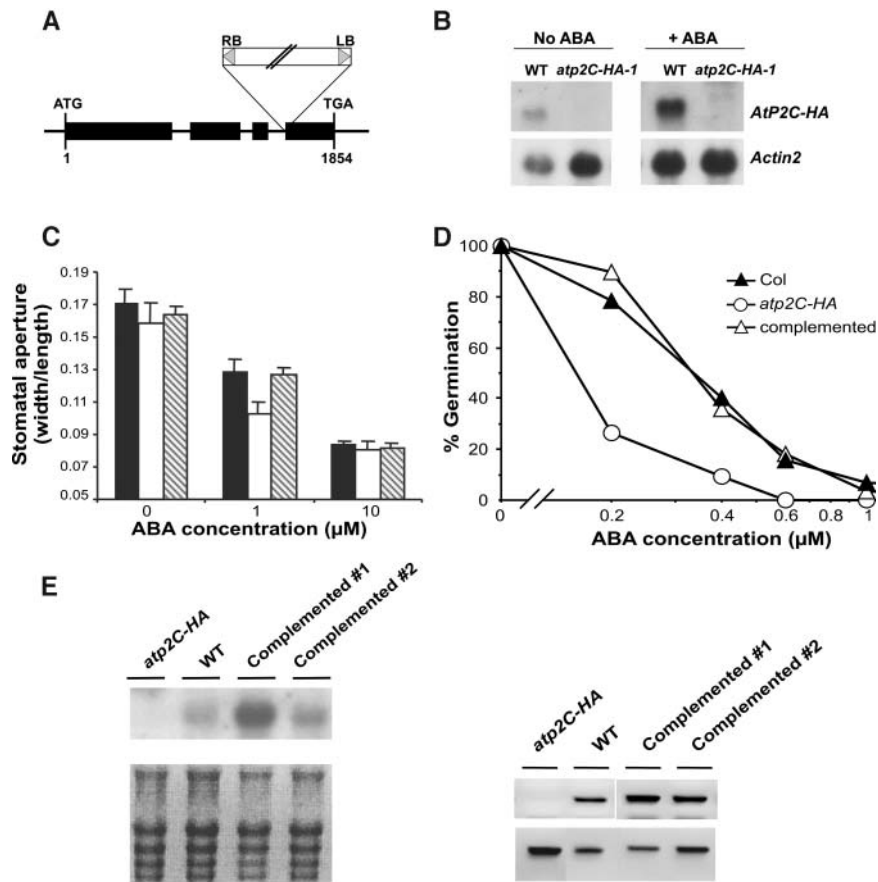
Figure 8. *atp2C-HA-1* Mutant Shows ABA Hypersensitivity in Stomatal Response and ABA Inhibition of Seed Germination.

(A) Genomic organization of *AtP2C-HA* gene. Exons are shown as boxes, whereas introns are shown as lines. The insertion site and orientation of the T-DNA in the *atp2C-HA-1* mutant are indicated.

(B) RNA gel blot confirms disruption of the *AtP2C-HA* mRNA in *atp2C-HA-1* mutant and ABA induction in the wild-type plants.

(C) Stomatal aperture measurements show that ABA-induced stomatal closing is ABA hypersensitive in the *atp2C-HA-1* T-DNA disruption mutant (open bars) compared with the wild type (black bars) and that the *AtP2C-HA* cDNA complemented this phenotype (hatched bars, line 1). Stomatal apertures were measured 3 h after addition of 0.01 or 0.1 μM ABA.

(D) The *atp2C-HA-1* (*atp2C-HA*) mutation causes ABA hypersensitivity in ABA inhibition of seed germination, which is complemented by the *AtP2C-HA* cDNA.

(E) RNA gel blots (left) and RT-PCR (right) show that *At2PC-HA* expression is restored in the *atp2C-HA-1* complemented lines. Bottom left, total RNA control; bottom right, actin 2 control. Error bars represent SE of $n = 6$ independent experiments with 240 stomata each analyzed for the wild type and *atp2C-HA-1* (*atp2C-HA*) and of two independent experiments with 80 stomata each analyzed for a complemented *atp2C-HA-1* (line 1) in **(C)** and >50 seeds at each data point in **(D)**.

The large number of multimember gene families found in plant genomes likely causes redundancies and partial redundancies, thus greatly limiting the number of genes that can be identified in conventional genetic mutant screens. Furthermore, knockout mutant analyses based on the many possible combinations of double or triple mutants of homologous genes are limited without knowledge of cell type–specific expression. In one of many possible examples, 10 NADPH oxidase genes are found in the Arabidopsis genome, giving rise to 45 possible double mutant combinations. We identified two ABA-induced NADPH oxidase *Atrboh* genes expressed at high levels in guard cells from the presented data sets. A double mutant in these two *AtrbohD* and *AtrbohF* genes shows ABA insensitivity in ABA activation of plasma membrane calcium permeable I_{Ca} channels (Kwak et al., 2003). In another example, assuming ≥69 PP2C genes found in Arabidopsis, ≥2346 distinct double mutant lines could be generated, and no recessive gene deletion mutant phenotypes have been reported previously for plant PP2Cs. Among 69 genes encoding PP2Cs in the whole genome of Arabidopsis, only four of those present on the array are highly expressed in guard cells. From our published findings using the guard cell expression data sets presented here, analyses of present genes (called Present by Affymetrix Microarray Suite 5.0 software) and selection, in particular, of highly expressed genes for functional genomic

analyses can lead to identification of new players and new mechanisms that mediate guard cell and/or ABA signal transduction (e.g., Figure 8; Kwak et al., 2003). This approach circumvents the redundancy problem in signal transduction. Moreover, this approach will also be valuable for characterizing the functions of many highly expressed genes that are presently annotated as of unknown function.

We identified the *AtP2C-HA* gene (Rodriguez et al., 1998) as one of the most strongly ABA-induced PP2C mRNA in guard cells and one of the most highly expressed among the PP2Cs. To determine whether AtP2C-HA may play a role in ABA signaling, we characterized a T-DNA disruption mutant *atp2C-HA-1*. The *atp2C-HA-1* mutant shows ABA-hypersensitive regulation of stomatal closing (Figure 8C) and seed germination (Figure 8D). The ABA hypersensitivity is complemented by the *AtP2C-HA* cDNA (Figures 8C and 8D). These findings suggest that AtP2C-HA is a component of ABA signaling, acting as a negative regulator of the analyzed ABA responses.

In conclusion, genomic scale cell type–specific expression profiling provides a powerful tool for narrowing down the genome and greatly facilitates the determination of the functions of highly expressed and ABA-regulated genes belonging to large gene families or to genes of unknown function in plants. The identification of an ABA-hypersensitive disruption mutant in the *AtP2C-HA* gene illustrates the power of this approach. These analyses allow focused cell type–dependent phenotypic and mechanistic characterizations.

METHODS

Plant Growth and ABA Treatment

Wild-type Arabidopsis plants, ecotype Columbia, were grown in soil in a plant growth chamber with a 16-h-light (80 μE light fluence rate) and 8-h-dark cycle at 20°C and 40% humidity. After 5 to 6 weeks, plants were sprayed with 100 μM ABA ($+/-$ *cis*,*trans* ABA; Sigma, St. Louis, MO) or with water 4 h before cell isolations at the same time of day, after 1 h light, to eliminate variation as a result of diurnal changes in gene expression. In addition, cell isolations from ABA-treated and control-treated plants were performed simultaneously to eliminate variation because of growth conditions.

Isolation of Guard Cell Protoplasts

Arabidopsis rosette leaves of $\sim$100 plants were excised and blended for 3 min with a Waring blender at room temperature in water in the presence of actinomycin D (33 mg/L) and cordycepin (100 mg/L). Epidermal fragments were collected and filtered through a nylon mesh (pore size 100 μm). To remove epidermal and mesophyll cells, epidermal peels from $\sim$1600 leaves were transferred into a flask containing 50 mL of 0.7% Cellulysin (Calbiochem, San Diego, CA), 0.01% polyvinylpyrrolidone 40, 0.25% BSA, 55% basic medium, pH 5.5, and incubated at 27°C in a linear shaking water bath in the dark. The basic medium contained 0.5 mM CaCl$_2$, 0.5 mM MgCl$_2$, 0.01% cordycepin, 0.0033% actinomycin D, 5 mM Mes, pH 5.5, and the osmolarity was adjusted to 500 mmol/kg by addition of D-sorbitol. After 3 h of incubation, epidermal fragments were examined under a microscope. If few mesophyll cells remained, incubation was continued for an additional 30 min. When all epidermal and mesophyll cells were digested, epidermal fragments were collected on a nylon mesh (pore size 100 μm) and rinsed two to three times with the basic medium.

After washing, epidermal fragments were transferred to a flask containing 50 mL of basic medium containing 1.5% Cellulase RS (Yakult, Tokyo, Japan), 0.03% Pectolyase Y23 (Seishin Pharmaceutical, Tokyo, Japan), 0.25% BSA (Sigma), 0.01% cordycepin (Sigma), 0.0033% actinomycin D (Sigma), pH 5.5, and incubated at 19°C in a shaking water bath (70 rpm) until guard cell protoplasts were released, usually after $\sim$2 h. The solution containing guard cell protoplasts was filtered through four layers of a nylon mesh (pore size 10 μm), and guard cell protoplasts were collected by centrifugation at 1000g for 5 min. This last step was repeated three to four times to keep guard cell protoplasts free from other cells or cell fragment contamination. Guard cells and mesophyll cells were collected simultaneously, and RNA was extracted, thus resulting in equal durations from leaf excision to RNA extractions for guard cells and mesophyll cells. Guard cell purity was determined using a hemacytometer. The guard cell protoplasts that showed a purity of $\sim$99% were selected for further experiments. To prevent changes of gene expression during protoplast isolation, two different transcription inhibitors, actinomycin D (33 mg/L) and cordycepin (100 mg/L), were used in all procedures of the isolation, including the first step of blending. Total RNA from guard cell protoplasts was then extracted using Trizol reagent according to the manufacturer's instructions (Life Technologies, Cleveland, OH). For each of the 18 independent guard cell RNA extractions, approximately 5 μg of total RNA were obtained from 10^9 guard cell protoplasts, which were from $\sim$100 plants.

Isolation of Mesophyll Cell Protoplasts

Five grams of rosette leaves were cut from Arabidopsis plants treated with ABA or water and placed in a Petri dish containing 0.5 mM CaCl$_2$, 0.5 mM MgCl$_2$, 5 mM MES, 1.5% Cellulase RS, 0.03% Pectolyase Y23, 0.25% BSA, actinomycin D (33 mg/L), and cordycepin (100 mg/L), pH 5.5. Osmolarity was adjusted to 550 mmol/kg by addition of D-sorbitol. Leaves were chopped with a sterile razor blade into small squares of 5 to 10 mm^2 and incubated for 2 h at room temperature in the dark with gentle agitation until mesophyll cell protoplasts were released. The protoplast suspension was filtered through a nylon mesh (30 μm), washed several times, and resuspended with the basic medium under the same shaking conditions (70 rpm) until guard cells were ready in parallel isolations (see above). Cell purity was examined by a hemacytometer, and total RNA was extracted using Trizol reagent.

GeneChip Microarray Experiments and Data Analyses

Ten micrograms of total RNA from three independent protoplast extractions were pooled and used for each DNA chip hybridization, representing a total of 30 independent RNA isolations. Affymetrix Gene-Chips (Santa Clara, CA) were used, representing $\sim$8100 Arabidopsis genes. The transcript population of guard cells and mesophyll cells treated by ABA or water was amplified, labeled, and hybridized at the University of California, Irvine, and University of California, San Diego Gene Chip Core facilities. For each condition (with or without ABA), two (mesophyll cell) or three (guard cell) independent hybridizations were performed. Control and ABA-treated plants were grown in parallel for each isolation. The isolations took place over a period of 18 months and showed reproducibility (Figure 2, see Supplemental Figure 1). A set of spiked biotin-labeled bacterial RNAs, all at varying total concentrations, was added to the samples at the time of hybridization and included in the overall intensity normalization. The data were first analyzed with Microarray Suite 5.0 software (Affymetrix). For each microarray, overall intensity normalization for the entire probe sets was performed using Affymetrix Microarray Suite 5.0. Using the GeneChip Suite 5.0 default parameters, the detection P-value and the signal value were calculated for each probe set from each independent guard cell and mesophyll cell hybridization.

The detection P-value generated by this analysis allowed us to determine whether a transcript is reliably detected (Present, P-value <0.04), and the signal value assigns a relative measure of abundance to the transcript. The data were then passed through a quality filter using Excel (Microsoft, Redmond, WA), through which transcripts were selected for further analyses according to the following ad hoc criteria: a significantly expressed transcript must have been significantly expressed in at least two samples obtained under the same condition (P for Present, detection P-value <0.04. In the case of guard cells, a third experiment call of M for Marginal was allowed, detection P-value <0.06 in Affymetrix nomenclature). Note that low abundance transcripts may actually encode important cellular proteins even if statistical analyses define these as Absent (A).

For the comparison analyses reported in the tables, in the study of ABA responses and cell type expression, each sample was compared with the corresponding control-treated sample from plants grown at the same times and samples isolated in parallel using Affymetrix Microarray Suite 5.0, which provides values as the $\log_2$ of the intensity ratio (signal $\log_2$ ratio). The signal $\log_2$ ratio corresponding to the change in expression level determined for each probe set was calculated by comparing each probe pair from one array to the corresponding probe pair on the other array. Then, using the signal $\log_2$ ratio value, we calculated the fold change for each probe set according to the following formula:

$$\text{If signal log ratio} \geq 0, \text{ fold change} = 2^{\text{signal log ratio}}$$

$$\text{If signal log ratio} < 0, \text{ fold change} = (-1) \cdot 2^{-(\text{signal log ratio})}$$

In addition, for all comparison analyses that we performed, the change P-value, measuring the probability that the expression levels of each probe set are different between two arrays, was calculated. When the change P-value is close to 0.5, they are likely to be the same. When the change P-value is close to 0, the expression level in the ABA-treated array is higher than that of the control array. When the change P-value is close to 1, the expression level in the ABA-treated array is lower than that of the control array (Affymetrix). Only probe sets that showed significant differences in the two independent comparison analyses for mesophyll cells or in the three independent comparison analyses for guard cells were selected.

To perform cluster analysis (Figure 5), the statistically normalized preselected data of each array were analyzed using GeneSpring 4.2 software (Silicon Genetics, Redwood, CA) as replicate for mesophyll cells and triplicate for guard cells, and a second type of normalization, a per-gene normalization, was applied across all experiments using algorithms implemented in the GeneSpring program. This normalization method, also referred to as normalizing to the median for each gene, is intended to remove the differing intensity scales and binding rates from multiple experimental readings, allowing comparisons of multiple GeneChip hybridizations. It normalizes each gene to itself, so the median of all of the measurements is 1 for each replicate or triplicate experiment. To calculate this, GeneSpring divides each gene's signal by the median of all the signals for that particular gene. This normalization allows comparison of the relative changes in gene expression levels and display of these levels on a similar scale on the same graph. The expression pattern clusters were predefined by subjecting the relative differential expression data set obtained as described above to K-means clustering algorithms (K = 6), as implemented in the GeneSpring program using the standard correlation distance definition.

Affymetrix probe identifiers were matched with Arabidopsis Genome Initiative (AGI) identifiers by Basic Local Alignment Search Tool analysis of the published target sequences against the Institute for Genomic Research (TIGR) ATH1 sequences. For ~5% of the detected transcripts, we were unable to unambiguously identify a gene in the ATH1 genome sequence corresponding to that probe set. These genes are listed in the tables as no hit. A full description of how we identified the AGI identifiers

for the probe sets is available at http://www-biology.ucsd.edu/labs/schroeder/index.html, click on Genechip (Ghassemian et al., 2001). Note that if less stringent matches are allowed for annotation of the Affymetrix probes, some of the no-hit probes listed in the tables may conceivably cross-hybridize with known genes (see supplemental data online, http://www-biology.ucsd.edu/labs/schroeder/index.html, and http://genetics.mgh.harvard.edu/sheenweb.html). In addition to the supplemental data online, the complete set of raw Excel data files from Affymetrix chip experiments have been deposited at http://www-biology.ucsd.edu/labs/schroeder/guardcellchips.html, allowing users to pursue additional analyses and to develop functional genomic applications in guard cells and mesophyll cells.

RT-PCR Analyses

The expression profiles obtained from chip hybridizations were further validated by RT-PCR using first-strand cDNA synthesized from independently isolated RNA samples. Two micrograms of total RNA was converted into cDNA. Each cDNA was diluted 50 times, and 1 μL of cDNA was used for 27 cycle three-step PCR. RT-PCR amplifications were performed with 29 genes that were preferentially expressed in guard cells and showed transcript level induction or repression in response to ABA preferentially in guard cells or in both cell types. The *Actin2* gene (forward primer, 5′-ggccgatggtgaggatattcagccacttg-3′; reverse primer, 5′-tcgatggacctgactcatcgtactcactc-3′) was used as a control for RT-PCR experiments. Guard cell preferentially expressed genes include a calcium-dependent protein kinase gene (forward primer, 5′-tggtagtgcatactatgtagc-3′; reverse primer, 5′-gacacaccatgtagcaat-3′) and *CER2* (forward primer, 5′-cataccttacattcgctgc-3′; reverse primer, 5′-actacacttacaatccttgc-3′). ABA-induced genes preferentially expressed in guard cells include a trehalose-6-phosphate synthase (forward primer, 5′-ggcttctaatcctgggt-3′; reverse primer, 5′-ggtggtcttcggtctc-3′) and a LEA (forward primer, 5′-gaggaaagtgtacggtttg-3′; reverse primer, 5′-cgtcatatcgctcgcc-3′). The *KAT1* gene (forward primer, 5′-ccgatcttctaccatctcttggagccagg-3′; reverse primer, 5′-agttgcagcctccaaacttctcacttgc-3′) is an ABA-repressed gene preferentially expressed in guard cells. ABA-induced genes in guard cells and mesophyll cells include a dehydrin (forward primer, 5′-aagattaaagagcaactgcc-3′; reverse primer, 5′-aacgaaaccagaagtagatatt-3′), the protein phosphatase *AtP2C-HA* (forward primer, 5′-taccgctttggggcac-3′; reverse primer, 5′-ggacctagacatggcga-3′), and *COR47* (forward primer, 5′-ctgaaccggagttagc-3′; reverse primer, 5′-cttggcatgataacctgga-3′). The following *AtP2C-HA* primers were used to confirm *AtP2C-HA* cDNA expression in the complemented lines: forward primer, 5′-atggaggagatgactcccgcagtt-3′; reverse primer, 5′-tcaggttctggtcttgaactttctt-3′.

Promoter Analyses

The upstream nucleotide sequences used were obtained from the file At.upstream.1000.20020107 obtained from the FTP site of the Arabidopsis Information Resource (TAIR; http://www.arabidopsis.org). A file of 500-bp sequences was derived from the above file by extracting 500 bp from the 3′ end of each sequence. The association between the Affymetrix probe sets and the AGI identifiers used to identify the sequences was determined by Basic Local Alignment Search Tool analysis of the Affymetrix target sequences against the TIGR nucleotide sequences. Stringent criteria were applied to matches (http://www-biology.ucsd.edu/labs/schroeder/howandwhy.html). We were able to unambiguously identify upstream sequences for 7749 of the genes on the GeneChip. Motif searches were performed by writing custom Python scripts (http://www.python.org) and C extensions, which search for both exact and approximate matches to a pattern. Both forward and reverse strands were searched, and some patterns

contained wildcard nucleotides (e.g., S = C or G, Y = pyrimidine). Because the degree of conservation of many of these patterns is unknown, each pattern was searched using criteria of 0 or 1 allowed mismatches (Table 4). The P-values given in the table are based on an upper tail hypergeometric cumulative distribution function and represent the probability of obtaining at least as many hits as were observed in the set, if the set were a random sample drawn without replacement from the complete set of promoter sequences. The equation used was:

$$P = 1 - \sum_{k=0}^{r-1} \frac{\binom{R}{k}\binom{N-R}{n-k}}{\binom{N}{n}},$$

where N = population size, R = number of hits in the population, n = sample size, and r = number of hits in the sample.

Stomatal Aperture Measurements

Leaves of 5- to 6-week-old wild type, *atp2C-HA*, and complemented *atp2C-HA-1* plants were used for stomatal aperture measurements. For Figure 8C, epidermal strips were peeled and incubated 2 h in white light in stomatal opening solution containing 10 mM KCl, 7.5 mM iminodiacetic acid, and 10 mM MES/Tris, pH 6.2, at 20°C.

Seed Germination Analyses

Seeds of the wild type and *atp2C-HA* were plated on Murashige and Skoog medium (Sigma) containing 0, 0.2, 0.4, 0.6, or 1 µM ABA. Seeds were stratified at 4°C for 4 d and then transferred to a growth chamber (24°C under 16-h-light/8-h-dark regime). Seed germination rates were scored after 6 d in the growth chamber. Germination is defined as the emergence of both cotyledons and roots from the seed.

Complementation of the *atp2C-HA-1* Mutant

A 1.54-kb fragment corresponding to the *AtP2C-HA* coding region was amplified by RT-PCR from Arabidopsis cDNA with forward (5′-ATC-CATGGAGGAGATGACTCCCGCAGTT-3′) and reverse (5′-TAGCTA-GCTCAGGTTCTGGTCTTGAACTTTCTT-3′) primers. The PCR product was digested with NcoI and NheI and cloned into the NcoI and PmlI sites of the binary vector pCAMBIA 1302 (CAMBIA, Canberra, Australia) to express the *AtP2C-HA* coding sequence under the 35S promoter of the *Cauliflower mosaic virus*. This construct was verified by DNA sequencing and transformed into the *atp2C-HA-1* mutant plants by the floral dip method using the *Agrobacterium tumefaciens* strain C58. Transgenic lines were selected on Murashige and Skoog medium containing 25 µg/mL hygromycin.

REFERENCES

Allen, G.J., Chu, S.P., Harrington, C.L., Schumacher, K., Hoffmann, T., Tang, Y.Y., Grill, E., and Schroeder, J.I. (2001). A defined range of guard cell calcium oscillation parameters encodes stomatal movements. Nature **411,** 1053–1057.

Allen, G.J., Murata, Y., Chu, S.P., Nafisi, M., and Schroeder, J.I. (2002). Hypersensitivity of abscisic acid-induced cytosolic calcium increases in the *Arabidopsis* farnesyltransferase mutant *era1–2*. Plant Cell **14,** 1649–1662.

Anderson, J.A., Huprikar, S.S., Kochian, L.V., Lucas, W.J., and Gaber, R.F. (1992). Functional expression of a probable *Arabidopsis thaliana* potassium channel in *Saccharomyces cerevisiae*. Proc. Natl. Acad. Sci. USA **89,** 3736–3740.

Bartholomew, D.M., Bartley, G.E., and Scolnik, P.A. (1991). Abscisic acid control of *rbcs* and *cab* transcription in tomato leaves. Plant Physiol. **96,** 291–296.

Becker, J.D., Boavida, L.C., Carneiro, J., Haury, M., and Feijo, J.A. (2003). Transcriptional profiling of Arabidopsis tissues reveals the unique characteristics of the pollen transcriptome. Plant Physiol. **133,** 713–725.

Bell, W., Sun, W.N., Hohmann, S., Wera, S., Reinders, A., De Virgilio, C., Wiemken, A., and Thevelein, J.M. (1998). Composition and functional analysis of the *Saccharomyces cerevisiae* trehalose synthase complex. J. Biol. Chem. **273,** 33311–33319.

Birnbaum, K., Shasha, D.E., Wang, J.Y., Jung, J.W., Lambert, G.M., Galbraith, D.W., and Benfey, P.N. (2003). A gene expression map of the Arabidopsis root. Science **302,** 1956–1960.

Blatt, M.R., and Armstrong, F. (1993). K$^+$ channels of stomatal guard cells: Abscisic-acid-evoked control of the outward rectifier mediated by cytoplasmic pH. Planta **191,** 330–341.

Busk, P.K., and Pages, M. (1998). Regulation of abscisic acid-induced transcription. Plant Mol. Biol. **37,** 425–435.

Chang, Y.C., and Walling, L.L. (1991). Abscisic acid negatively regulates expression of chlorophyll a/b binding protein genes during soybean embryogeny. Plant Physiol. **97,** 1260–1264.

Chen, W.Q., et al. (2002). Expression profile matrix of *Arabidopsis* transcription factor genes suggests their putative functions in response to environmental stresses. Plant Cell **14,** 559–574.

Cherel, I., Michard, E., Platet, N., Mouline, K., Alcon, C., Sentenac, H., and Thibaud, J.B. (2002). Physical and functional interaction of the *Arabidopsis* K$^+$ channel AKT2 and phosphatase AtPP2CA. Plant Cell **14,** 1133–1146.

Cutler, S., Ghassemian, M., Bonetta, D., Cooney, S., and McCourt, P. (1996). A protein farnesyl transferase involved in abscisic acid signal transduction in *Arabidopsis*. Science **273,** 1239–1241.

Finkelstein, R.R. (1994). Mutations at two new *Arabidopsis* ABA response loci are similar to *abi3* mutations. Plant J. **5,** 765–771.

Finkelstein, R.R., Gampala, S.S.L., and Rock, C.D. (2002). Abscisic acid signaling in seeds and seedlings. Plant Cell **14,** S15–S45.

Finkelstein, R.R., and Lynch, T.J. (2000). The *Arabidopsis* abscisic acid response gene *ABI5* encodes a basic leucine zipper transcription factor. Plant Cell **12,** 599–609.

Gazzarrini, S., and McCourt, P. (2001). Genetic interactions between ABA, ethylene and sugar signaling pathways. Curr. Opin. Plant Biol. **4,** 387–391.

Ghassemian, M., Waner, D., Tchieu, J., Gribskov, M., and Schroeder, J.I. (2001). An integrated *Arabidopsis* annotation database for Affymetrix Genechip[(R)] data analysis, and tools for regulatory motif searches. Trends Plant Sci. **6,** 448–449.

Gilmour, S.J., Artus, N.N., and Thomashow, M.F. (1992). cDNA sequence analysis and expression of two cold-regulated genes of *Arabidopsis thaliana*. Plant Mol. Biol. **18,** 13–22.

Giraudat, J., Hauge, B.M., Valon, C., Smalle, J., Parcy, F., and Goodman, H.M. (1992). Isolation of the *Arabidopsis ABI3* gene by positional cloning. Plant Cell **4,** 1251–1261.

Harmer, S.L., Hogenesch, J.B., Straume, M., Chang, H.-S., Han, B., Zhu, T., Wang, X., Kreps, J.A., and Kay, S.A. (2000). Orchestrated

transcription of key pathways in *Arabidopsis* by the circadian clock. Science **290,** 2110–2113.

Honys, D., and Twell, D. (2003). Comparative analysis of the *Arabidopsis* pollen transcriptome. Plant Physiol. **132,** 640–652.

Hoth, S., Morgante, M., Sanchez, J.P., Hanafey, M., Tingey, S., and Chua, N.-H. (2002). Genome-wide gene expression profiling in *Arabidopsis thaliana* reveals new targets of abscisic acid and largely impaired gene regulation in the *abi1–1* mutant. J. Cell Sci. **115,** 4891–4900.

Hughes, J.D., Estep, P.W., Tavazoie, S., and Church, G.M. (2000). Computational identification of *cis*-regulatory elements associated with groups of functionally related genes in *Saccharomyces cerevisiae*. J. Mol. Biol. **296,** 1205–1214.

Hugouvieux, V., Kwak, J.M., and Schroeder, J.I. (2001). An mRNA cap binding protein, ABH1, modulates early abscisic acid signal transduction in *Arabidopsis*. Cell **106,** 477–487.

The International Human Genome Mapping Consortium. (2001). A physical map of the human genome. Nature **409,** 934–941.

Kiyosue, T., Yamaguchi-Shinozaki, K., and Shinozaki, K. (1994). Characterization of two cDNAs (*ERD10* and *ERD14*) corresponding to genes that respond rapidly to dehydration stress in *Arabidopsis thaliana*. Plant Cell Physiol. **35,** 225–231.

Kwak, J.M., Kim, S.A., Hong, S.W., and Nam, H.G. (1997). Evaluation of 515 expressed sequence tags obtained from guard cells of *Brassica campestris*. Planta **202,** 9–17.

Kwak, J.M., Moon, J.-H., Murata, Y., Kuchitsu, K., Leonhardt, N., DeLong, A., and Schroeder, J.I. (2002). Disruption of a guard cell-expressed protein phosphatase 2A regulatory subunit, *RCN1*, confers abscisic acid insensitivity in *Arabidopsis*. Plant Cell **14,** 2849–2861.

Kwak, J.M., Mori, I.C., Pei, Z.-M., Leonhardt, N., Torres, M.A., Dangl, J.L., Bloom, R.E., Bodde, S., Jones, J.D.G., and Schroeder, J.I. (2003). NADPH oxidase *AtrbohD* and *AtrbohF* genes function in ROS-dependent ABA signaling in *Arabidopsis*. EMBO J. **22,** 2623–2633.

Lee, H., Xiong, L., Gong, Z., Ishitani, M., Stevenson, B., and Zhu, J.-K. (2001). The *Arabidopsis HOS1* gene negatively regulates cold signal transduction and encodes a RING finger protein that displays cold-regulated nucleo-cytoplasmic partitioning. Genes Dev. **15,** 912–924.

Lemtiri-Chlieh, F. (1996). Effects of internal K$^+$ and ABA on the voltage- and time-dependence of the outward K$^+$-rectifier in *Vicia* guard cells. J. Membr. Biol. **153,** 105–116.

Lemtiri-Chlieh, F., and MacRobbie, E.A.C. (1994). Role of calcium in the modulation of *Vicia* guard cell potassium channels by abscisic acid: A patch-clamp study. J. Membr. Biol. **137,** 99–107.

Leung, J., Merlot, S., and Giraudat, J. (1997). The *Arabidopsis ABSCISIC ACID-INSENSITIVE2* (*ABI2*) and *ABI1* genes encode homologous protein phosphatases 2C involved in abscisic acid signal transduction. Plant Cell **9,** 759–771.

Li, J., Kinoshita, T., Pandey, S., Ng, C.K.-Y., Gygi, S.P., Shimazaki, K.-I., and Assmann, S.M. (2002). Modulation of an RNA-binding protein by abscisic-acid-activated protein kinase. Nature **418,** 793–797.

Lopez-Molina, L., and Chua, N.-H. (2000). A null mutation in a bZIP factor confers ABA-insensitivity in *Arabidopsis thaliana*. Plant Cell Physiol. **41,** 541–547.

Lu, C., and Fedoroff, N. (2000). A mutation in the *Arabidopsis HYL1* gene encoding a dsRNA binding protein affects responses to abscisic acid, auxin, and cytokinin. Plant Cell **12,** 2351–2366.

MacRobbie, E.A.C. (1998). Signal transduction and ion channels in guard cells. Phil. Trans. Roy. Soc. London **1374,** 1475–1488.

Mäser, P., Leonhardt, N., and Schroeder, J.I. (2003). The clickable guard cell: Electronically linked model of guard cell signal transduction pathways. In The Arabidopsis Book, http://www-biology.ucsd.edu/labs/schroeder/clickablegc.html.

Merlot, S., Gosti, F., Guerrier, D., Vavasseur, A., and Giraudat, J. (2001). The ABI1 and ABI2 protein phosphatases 2C act in a negative feedback regulatory loop of the abscisic acid signalling pathway. Plant J. **25,** 295–303.

Murata, Y., Pei, Z.-M., Mori, I.C., and Schroeder, J.I. (2001). Abscisic acid activation of plasma membrane Ca^{2+} channels in guard cells requires cytosolic NAD(P)H and is differentially disrupted upstream and downstream of reactive oxygen species production in *abi1–1* and *abi2–1* protein phosphatase 2C mutants. Plant Cell **13,** 2513–2523.

Mustilli, A.-C., Merlot, S., Vavasseur, A., Fenzi, F., and Giraudat, J. (2002). Arabidopsis OST1 protein kinase mediates the regulation of stomatal aperture by abscisic acid and acts upstream of reactive oxygen species production. Plant Cell **14,** 3089–3099.

Nakamura, R.L., McKendree, W.L., Hirsch, R.E., Sedbrook, J.C., Gaber, R.F., and Sussman, M.R. (1995). Expression of an *Arabidopsis* potassium channel gene in guard cells. Plant Physiol. **109,** 371–374.

Nylander, M., Svensson, J., Palva, E.T., and Welin, B.V. (2001). Stress-induced accumulation and tissue-specific localization of dehydrins in *Arabidopsis thaliana*. Plant Mol. Biol. **45,** 263–279.

Okamura, J.K., and Goldberg, R.B. (1989). Regulation of plant gene expression: General principles. In The Biochemistry of Plants, Vol. 115, P.K. Stumpf and E.E. Conn, eds (New York, NY: Academic Press), pp. 1–82.

Ozturk, Z.N., Talame, V., Deyholos, M., Michalowski, C.B., Galbraith, D.W., Gozukirmizi, N., Tuberosa, R., and Bohnert, H.J. (2002). Monitoring large-scale changes in transcript abundance in drought- and salt-stressed barley. Plant Mol. Biol. **48,** 551–573.

Pei, Z.-M., Ghassemian, M., Kwak, C.M., McCourt, P., and Schroeder, J.I. (1998). Role of farnesyltransferase in ABA regulation of guard cell anion channels and plant water loss. Science **282,** 287–290.

Pei, Z.-M., Kuchitsu, K., Ward, J.M., Schwarz, M., and Schroeder, J.I. (1997). Differential abscisic acid regulation of guard cell slow anion channels in *Arabidopsis* wild-type and *abi1* and *abi2* mutants. Plant Cell **9,** 409–423.

Pei, Z.-M., Murata, Y., Benning, G., Thomine, S., Klusener, B., Allen, G.J., Grill, E., and Schroeder, J.I. (2000). Calcium channels activated by hydrogen peroxide mediate abscisic acid signalling in guard cells. Nature **406,** 731–734.

Perez-Amador, M.A., Lidder, P., Johnson, M.A., Landgraf, J., Wisman, E., and Green, P.J. (2001). New molecular phenotypes in the *dst* mutants of *Arabidopsis* revealed by DNA microarray analysis. Plant Cell **13,** 2703–2717.

Reinbothe, S., Reinbothe, C., and Parthier, B. (1993). Methyl jasmonate represses translation initiation of a specific set of mRNAs in barley. Plant J. **4,** 459–467.

Rodriguez, P.L., Benning, G., and Grill, E. (1998). ABI2, a second protein phosphatase 2C involved in abscisic acid signal transduction in *Arabidopsis*. FEBS Lett. **421,** 185–190.

Romero, C., Belles, J.M., Vaya, J.L., Serrano, R., and Culianezmacia, F.A. (1997). Expression of the yeast trehalose-6-phosphate synthase gene in transgenic tobacco plants: Pleiotropic phenotypes include drought tolerance. Planta **201,** 293–297.

Schachtman, D., Schroeder, J.I., Lucas, W.J., Anderson, J.A., and Gaber, R.F. (1992). Expression of an inward-rectifying potassium channel by the *Arabidopsis KAT1* cDNA. Science **258,** 1654–1658.

Schena, M., Shalon, D., Davis, R.W., and Brown, P.O. (1995). Quantitative monitoring of gene expression patterns with a complementary DNA microarray. Science **270,** 467–470.

Schroeder, J.I., Kwak, J.M., and Allen, G.J. (2001). Guard cell abscisic acid signalling and engineering drought hardiness in plants. Nature **410,** 327–330.

Schwartz, A., Wu, W.-H., Tucker, E.B., and Assmann, S.M. (1994). Inhibition of inward K$^+$ channels and stomatal response by abscisic acid: An intracellular locus of phytohormone action. Proc. Natl. Acad. Sci. USA **91,** 4019–4023.

Seki, M., et al. (2002). Monitoring the expression pattern of around 7,000 *Arabidopsis* genes under ABA treatments using a full-length cDNA microarray. Funct. Integr. Genomics **2,** 282–291.

Seki, M., Narusaka, M., Abe, H., Kasuga, M., Yamaguchi-Shinozaki, K., Carninci, P., Hayashizaki, Y., and Shinozaki, K. (2001). Monitoring the expression pattern of 1300 *Arabidopsis* genes under drought and cold stresses by using a full-length cDNA microarray. Plant Cell **13,** 61–72.

Sheen, J., Zhou, L., and Jang, J.C. (1999). Sugars as signaling molecules. Curr. Opin. Plant Biol. **2,** 410–418.

Shinozaki, K., and Yamaguchi-Shinozaki, K. (2000). Molecular responses to dehydration and low temperature: Differences and cross-talk between two stress signaling pathways. Curr. Opin. Plant Biol. **3,** 217–223.

Wang, R.C., Guegler, K., LaBrie, S.T., and Crawford, N.M. (2000). Genomic analysis of a nutrient response in *Arabidopsis* reveals diverse expression patterns and novel metabolic and potential regulatory genes induced by nitrate. Plant Cell **12,** 1491–1509.

Wang, X.-Q., Ullah, H., Jones, A.M., and Assmann, S.M. (2001). G protein regulation of ion channels and abscisic acid signaling in *Arabidopsis* guard cells. Science **292,** 2070–2072.

Wanner, L.A., Li, G.Q., Ware, D., Somssich, I.E., and Davis, K.R. (1995). The phenylalanine ammonia-lyase gene family in *Arabidopsis thaliana*. Plant Mol. Biol. **27,** 327–338.

Weatherwax, S.C., Ong, M.S., Degenhardt, J., Bray, E.A., and Tobin, E.M. (1996). The interaction of light and abscisic acid in the regulation of plant gene expression. Plant Physiol. **111,** 363–370.

Wilhelm, K.S., and Thomashow, M.F. (1993). Arabidopsis thaliana cor15b, an apparent homologue of cor15a, is strongly responsive to cold and ABA, but not drought. Plant Mol. Biol. **25,** 1073–1077.

Xia, Y.J., Nikolau, B.J., and Schnable, P.S. (1997). Developmental and hormonal regulation of the *Arabidopsis CER2* gene that codes for a nuclear-localized protein required for the normal accumulation of cuticular waxes. Plant Physiol. **115,** 925–937.

Xiong, L., Gong, Z., Rock, C.D., Subramanian, S., Guo, Y., Xu, W., Galbraith, D., and Zhu, J.-K. (2001a). Modulation of abscisic acid signal transduction and biosynthesis by an Sm-like protein in *Arabidopsis*. Dev. Cell **1,** 771–781.

Xiong, L., Lee, B.-H., Ishitani, M., Lee, H., Zhang, C., and Zhu, J.-K. (2001b). *FIERY1* encoding an inositol polyphosphate 1-phosphatase is a negative regulator of abscisic acid and stress signaling in *Arabidopsis*. Genes Dev. **15,** 1971–1984.

Yamaguchi-Shinozaki, K., and Shinozaki, K. (1993). Characterization of the expression of a desiccation-response *RD29* gene of *Arabidopsis thaliana* and analysis of its promoter in transgenic plants. Mol. Gen. Genet. **236,** 331–340.

Yin, Y.H., Wang, Z.Y., Mora-Garcia, S., Li, J.M., Yoshida, S., Asami, T., and Chory, J. (2002). BES1 accumulates in the nucleus in response to brassinosteroids to regulate gene expression and promote stem elongation. Cell **109,** 181–191.

Yoshida, R., Hobo, T., Ichimura, K., Mizoguchi, T., Takahashi, F., Alonso, J., Ecker, J.R., and Shinozaki, K. (2002). ABA-activated *SnRK2* protein kinase is required for dehydration stress signaling in *Arabidopsis*. Plant Cell Physiol. **43,** 1473–1483.

Zhu, T., Budworth, P., Han, B., Brown, D., Chang, H.-S., Zou, G., and Wang, X. (2001). Toward elucidating the global gene expression patterns of developing *Arabidopsis*: Parallel analysis of 8300 genes by a high-density oligonucleotide probe array. Plant Physiol. Biochem. **39,** 221–242.

Zhu, J., Gong, Z., Zhang, C., Song, C.-P., Damsz, B., Inan, G., Koiwa, H., Zhu, J.-K., Hasegawa, P.M., and Bressan, R.A. (2002). OSM1/SPY61: A syntaxin protein in *Arabidopsis* controls abscisic acid–mediated and non-abscisic acid–mediated responses to abiotic stress. Plant Cell **14,** 3009–3028.